UNCLASSIFIED

SECURITY CLASSIFICATION OF THIS PAGE (When Data Entered)

DTIC FILE COPY

AD-A196 474

REPORT DOCUMENTATION PAGE		READ INSTRUCTIONS BEFORE COMPLETING FORM
1. REPORT NUMBER AFIT/CI/NR 88- 82	2. GOVT ACCESSION NO.	3. RECIPIENT'S CATALOG NUMBER
4. TITLE (and Subtitle) AVALANCHE CHARACTERISTICS OF SILICIDE SCHOTTKY BARRIER DIODES		5. TYPE OF REPORT & PERIOD COVERED MS THESIS 6. PERFORMING ORG. REPORT NUMBER
7. AUTHOR(s) KENNETH LEE YATES		8. CONTRACT OR GRANT NUMBER(s)
9. PERFORMING ORGANIZATION NAME AND ADDRESS AFIT STUDENT AT: UNIVERSITY OF ARIZONA		10. PROGRAM ELEMENT, PROJECT, TASK AREA & WORK UNIT NUMBERS
11. CONTROLLING OFFICE NAME AND ADDRESS		12. REPORT DATE 1988 13. NUMBER OF PAGES 56
14. MONITORING AGENCY NAME & ADDRESS(if different from Controlling Office) AFIT/NR Wright-Patterson AFB OH 45433-6583		15. SECURITY CLASS. (of this report) UNCLASSIFIED 15a. DECLASSIFICATION/DOWNGRADING SCHEDULE

16. DISTRIBUTION STATEMENT (of this Report)

DISTRIBUTED UNLIMITED: APPROVED FOR PUBLIC RELEASE

DTIC ELECTE AUG 0 4 1988 S C D

17. DISTRIBUTION STATEMENT (of the abstract entered in Block 20, if different from Report)

SAME AS REPORT

18. SUPPLEMENTARY NOTES

Approved for Public Release: IAW AFR 190-1
LYNN E. WOLAVER Lynn Wolaver 19 July 88
Dean for Research and Professional Development
Air Force Institute of Technology
Wright-Patterson AFB OH 45433-6583

19. KEY WORDS (Continue on reverse side if necessary and identify by block number)

20. ABSTRACT (Continue on reverse side if necessary and identify by block number)

ATTACHED

DD FORM 1 JAN 73 1473 EDITION OF 1 NOV 65 IS OBSOLETE

UNCLASSIFIED

SECURITY CLASSIFICATION OF THIS PAGE (When Data Entered)

ABSTRACT

This thesis investigates the use of an avalanche Platinum Silicide (PtSi) Schottky Barrier Diode as a detector in fiber optic communication systems for the 1.3 to 1.5 μm spectral region. The avalanche process is used to amplify the signal prior to electrical interfacing in order to enhance the signal-to-noise ratio.

The proper environment for avalanche use is when the system is pre amplifier noise limited. The amount of multiplication is predicted by the impact ionization coefficients for electrons and holes, α and β, respectively. Detectors should be constructed of materials where α and β differ greatly, and then the multiplication should be initiated by the carrier with the higher ionization coefficient. By using PtSi Schottky diodes, where $\alpha > \beta$, pure electron injection can be accomplished by irradiating with photons of energy $\psi < h\nu < E_g$ (where ψ is the Schottky Barrier height and E_g is the bandgap of silicon), thus maximizing multiplication and minimizing noise.

Experimental results on the PtSi diodes studied showed high dark currents at room temperature and premature reverse breakdown which prevented multiplication. However, values from previous reported results allow us to predict a multiplication of 68 with an excess-noise factor of 11.1, an NEP of 2.5×10^{-8} watts, and finally a gain-bandwidth product of 242 GHz.

An alternative means for avalanching involves the quantum effects of impurity-band ionization. By using a heavily doped semiconductor (10^{17} cm^{-3}) and operating at low temperatures ($T \cong 10^{0}K$), one can achieve noise-free gain at lower electric field strengths.

AVALANCHE CHARACTERISTICS OF SILICIDE SCHOTTKY BARRIER DIODES

by

Kenneth Lee Yates

A Thesis Submitted to the Faculty of the

COMMITTEE ON OPTICAL SCIENCES (GRADUATE)

In Partial Fulfillment of the Requirements

For the Degree of

MASTER OF SCIENCE

In the Graduate College

THE UNIVERSITY OF ARIZONA

1 9 8 7

STATEMENT BY AUTHOR

This thesis has been submitted in partial fulfillment of requirements for an advanced degree at The University of Arizona and is deposited in the University Library to be made available to borrowers under rules of the Library.

Brief quotations from this thesis are allowable without special permission, provided that accurate acknowledgement of source is made. Request for permission for extended quotation from or reproduction of this manuscript in whole or in part may be granted by the head of the major department or the Dean of the Graduate College when in his or her judgement the proposed use of the material is in the interests of scholarship. In all other instances, however, permission must be obtained from the author.

SIGNED: Kenneth L Yates

APPROVAL BY THESIS DIRECTOR

This thesis has been approved on the date shown below:

E. L. Dereniak
E. L. Dereniak
Associate Professor of Optical Sciences

Nov 20, 1987
Date

ACKNOWLEDGMENTS

I would like to express my gratitude to the faculty and staff of the Optical Sciences Center for providing the opportunity to further my education in optics. You have made my time at the Center productive and enjoyable.

I am grateful to Doctor Andy Yang and the Rome Air Development Center's Electronic Device Technology Division for providing the PtSi diodes and sharing their expertise in the field. I am also grateful to Mark Gramer at Litton Electronic Devices for performing the wire bonding work on the diodes.

Many thanks to Doctor Eustace L. Dereniak for his expertise, support, and guidance as my research advisor for this project.

Finally, I wish to dedicate my work to my wife, Conchita, without whose support, understanding, and love I would never have accomplished my research.

TABLE OF CONTENTS

LIST OF FIGURES v

ABSTRACT vii

1 INTRODUCTION 1

2 BACKGROUND AND THEORY OF THE SCHOTTKY BARRIER DIODE . . . 2

1 Historical Development 2
2 The Schottky Barrier 2
3 Current Transport Theory 5

3 AVALANCHE MULTIPLICATION 9

1 Background 9
2 Signal-to-Noise Analysis 9
3 Avalanche Gain Mechanism 14
4 Gain-Bandwidth Product 19
5 Maximum Multiplication 20
6 Excess-Noise Factor 21
7 Linearity and Frequency Response 25
8 Examples of Avalanche Detector Structures 27
9 Impurity Band Conduction 30

4 EXPERIMENTAL ARRANGEMENTS FOR PtSi INVESTIGATION 33

1 Platinum Silicide Diodes 33
2 Measurements Performed 35

5 EXPERIMENTAL RESULTS 41

6 CONCLUSIONS 53

REFERENCES 55

LIST OF FIGURES

Figure		Page
1.	Energy band diagrams of metal and semiconductor before (a) and after (b) contact	3
2.	Schottky diode showing interfaces where scattering can occur	8
3.	Block diagram showing the avalanche process (after Anderson, et al ref. 27)	10
4.	Signal-to-noise power increase as a function of multiplication	13
5.	Boundary conditions and electric field direction (after Stillman and Wolfe ref. 14)	16
6.	Electron multiplication as a function of electric field with various values of k (after Webb, et al ref. 15)	18
7.	I-V curves showing high versus low differential resistance	22
8.	Excess-noise factor versus multiplication (after Stillman and Wolfe ref. 14)	24
9.	Excess-noise factor versus multiplication for various fractions of injected electrons (after Webb, et al ref. 15)	26
10.	Energy diagram showing separate electron and hole injection by selection of wavelength (after Woods, et al ref. 21)	29
11.	Impurity-band impact ionization process	31
12.	Top and crossectional views of PtSi diode supplied by Hanscom AFB (RADC)	34
13.	Transimpedance amplifier circuit with reverse bias for detector readout	36
14.	Power incident on detector versus wavelength	38
15.	Test set up for measuring responsivity and multiplication	39
16.	I-V curves for various PtSi diodes	42
17.	Reverse saturation current for diodes a, e, and f (ref. figure 16)	43
18.	Dark current for diode f at T=85 K and room temperature	45
19.	Fowler plot showing barrier height of PtSi diode	46
20.	Responsivity and quantum efficiency versus wavelength diode e	47

21. Multiplication versus reverse bias for PtSi diode f 49

22. Fn versus Mn for predicted performance of PtSi diodes 52

ABSTRACT

This thesis investigates the use of an avalanche Platinum Silicide (PtSi) Schottky Barrier Diode as a detector in fiber optic communication systems for the 1.3 to 1.5 μm spectral region. The avalanche process is used to amplify the signal prior to electrical interfacing in order to enhance the signal-to-noise ratio.

The proper environment for avalanche use is when the system is pre amplifier noise limited. The amount of multiplication is predicted by the impact ionization coefficients for electrons and holes, α and β, respectively. Detectors should be constructed of materials where α and β differ greatly, and then the multiplication should be initiated by the carrier with the higher ionization coefficient. By using PtSi Schottky diodes, where $\alpha > \beta$, pure electron injection can be accomplished by irradiating with photons of energy $\psi < h\nu < E_g$ (where ψ is the Schottky Barrier height and E_g is the bandgap of silicon), thus maximizing multiplication and minimizing noise.

Experimental results on the PtSi diodes studied showed high dark currents at room temperature and premature reverse breakdown which prevented multiplication. However, values from previous reported results allow us to predict a multiplication of 68 with an excess-noise factor of 11.1, an NEP of 2.5×10^{-8} watts, and finally a gain-bandwidth product of 242 GHz.

An alternative means for avalanching involves the quantum effects of impurity-band ionization. By using a heavily doped semiconductor (10^{17} cm^{-3}) and operating at low temperatures ($T \cong 10^{0}K$), one can achieve noise-free gain at lower electric field strengths.

CHAPTER 1

INTRODUCTION

In recent years, research in the area of infrared detectors has concentrated on developing technology for use in optical communication systems.[1,2] To take advantage of the low attenuation $\left[\text{for example } 0.2 \frac{\text{dB}}{\text{km}} \text{ loss at } 1.55\ \mu\text{m}\right]$ and minimum dispersion of the fiber optics, one is required to operate in the 1.3 to 1.6 micron spectral region. However, this region is beyond the long wavelength cutoff of standard silicon detectors, and below long wavelength detectors made from extrinsic silicons. Because of this lack of detector technology, the Solid State Sciences Division, Rome Air Development Center at Hanscom Air Force Base, initiated research in the use of Schottky Barrier Diodes (SBD) as a possible candidate for this spectral region. In particular, the investigation has centered on Platinum Silicide (PtSi) Schottky diodes operated as avalanche detectors. This work will summarize the theory of operation of the SBD, investigate the principles of the avalanche multiplication process in solid state devices, explain the experimental technique used to evaluate the PtSi diodes, and finally analyze the test results and predict the SBD's usefullness as an optical communication detector.

CHAPTER 2

BACKGROUND AND THEORY OF THE SCHOTTKY BARRIER DIODE

Historical Development

The Schottky Barrier Diode is described as a metal-semiconductor contact. Early investigations found in literature include Braun in 1874[3] and a patented application as early as 1904.[4] In the 1930's work began on explaining the theory behind the device operation. In 1931 Wilson investigated the transport theory of semiconductors[5] and in 1938 Schottky formulated his theory on the existance of a potential barrier formed at the interface of the metal-semiconductor.[6] Although the theory of the Schottky barrier has now been studied for several decades, it was not until the introduction of Infrared Charge Coupled Device (IRCCD) imagers in the 1970's that the Schottky Barrier Diode as an infrared photodetector began to receive great attention. The two primary reasons for their attractiveness are 1) their compatibility with existing integrated circuit technology (ie. monolithic constructions) and 2) their low nonuniformity in pixel-to-pixel photoresponse.[7] For this study we are primarily interested in their spectral response and avalanche characteristics in the 1.3 to 1.6 μm region. But the ideal of monolithic construction makes the SBD an appealing detector for high volume - low cost production.

The Schottky Barrier

As briefly mentioned, a potential barrier is formed when a metal is brought into contact with a semiconductor. This has become known as the Schottky barrier and its theory is well explained by several books (for example S.M. Sze[8]). The mathematical description for the junction formed is very similar to that of a one-sided abrupt p-n junction. We are interested in the description of the barrier because it determines the spectral response of the detector. Figure 1 helps explain the formation of the barrier.

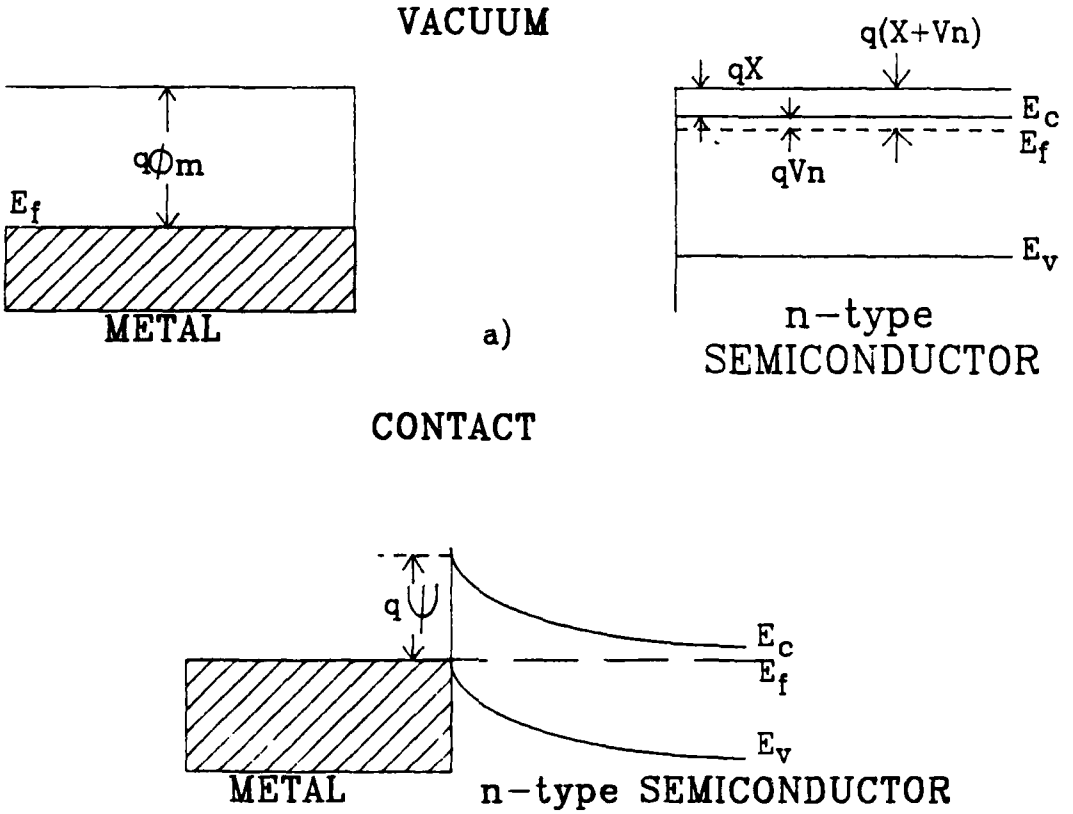

Figure 1. Energy band diagrams of metal and semiconductor before (a) and after (b) contact.

The Fermi levels, E_f , of the metal and semiconductor must line up when the two come in contact and thermal equilibrium is established. In the case of n-type silicon for example, the Fermi level in the semiconductor is lowered by an amount equal to the difference between the work functions of the metal and silicon. The work function is defined as the "energy difference between the vacuum level and the Fermi level,"[8] and is denoted by $q\phi_m$ for the metal and $q(\chi+V_n)$ for the semiconductor (see figure 1a), where

$q\chi$ = electron affinity measured from bottom of conduction band (E_c) to vacuum, and

$$qV_n = E_c - E_f .$$

As the gap between the metal and semiconductor approaches inter-atomic distances, the limiting case for formation of the barrier height in the absence of an external electric field is reached (see figure 1b), which is given by

$$q\psi_{Bn} = q(\phi_m - \chi), \qquad 2.1$$

the difference between the metal work function and electron affinity in the semiconductor. The above equation suggests that the barrier height is dependent only on the work function of the materials. This is true only for the case in which there is an absence of surface states. If surface states are present, then the barrier height is independent of the metal work function[8] and is given by

$$q\psi_{Bn} = E_g - q\phi_o \qquad 2.2$$

where $q\phi_o$ is the energy level at the surface coincident with the Fermi level prior to metal-semiconductor contact.

The barrier height is important because it determines the spectral response of the detector. An infrared photon absorbed in the metal will create electron-hole pairs by the process of internal photoemission. Only those electrons with energy greater than

the barrier height will cross over into the n-type semiconductor and be available for detection by an external circuit. Thus the barrier height determines the long wavelength cutoff, given by,

$$\lambda_{max} = \frac{1.24}{\psi_{Bn}} \qquad 2.3$$

When an external electric field is applied, an additional term appears in equations 2.1 - 2.2 due to the Schottky effect. Simply stated, the introduction of an electric field causes the Schottky barrier to be lowered by[8]

$$\Delta\phi = \sqrt{\frac{q\xi}{4\pi\epsilon_o}} \text{ in volts} \qquad 2.4$$

where

ξ = electric field in $\frac{V}{cm}$, and

ϵ_o = permittivity in free space.

The location of the barrier lowering from the metal surface is given by

$$x_m = \sqrt{\frac{q}{16\pi\xi\epsilon_o}} \text{ in cm.} \qquad 2.5$$

Equations 2.1 and 2.2 now become

$$q\psi_{Bn} = q(\phi_m - \chi) - q\Delta\phi \qquad 2.6$$

$$q\psi_{Bn} = E_g - q\phi_o - q\Delta\phi \qquad 2.7$$

Biasing the junction will also produce other effects similar to those seen in p-n junctions. For example, a reverse bias will widen the depletion region and decrease the capacitance, and therefore should increase the frequency response of the detector.[9]

Current Transport Theory

Completely describing the process of current transportation in Schottky diodes is an immense task and is beyond the scope of this work. Instead, those ideals that apply to the basic operation of the diode, and in particular the avalanche characteristics of the diode are presented. The four major processes are 1) electrons traversing

the Schottky barrier, 2) quantum mechanical tunneling through the barrier, 3) recombination in the space-charge region, and 4) hole injection from the metal into the semiconductor. One is primarily concerned with the first process because at low doping concentrations ($N_D < 10^{17}$ cm^{-3}), process one is dominant, while process two dominates at high doping concentrations and low temperatures.[8] We are also interested in leakage currents that manifest themselves as dark current, because the PtSi SBD's investigated have been fabricated with guard rings which are suppose to reduce these contributions to the dark current.

For high-mobility semiconductors like Si, the current transport over the barrier can be described by thermomic emission,

$$J_n = J_{ST}\left[\exp\left(\frac{qV}{nkT}\right) - 1\right] \qquad 2.8$$

where

J_n = current density in $\frac{A}{cm^2}$

n= ideality factor

J_{ST} = saturation current density

$$= A^* T^2 \exp\left(-\frac{q\psi_{Bn}}{kT}\right)$$

and A^* is the effective Richardson constant equal to 120 $\frac{A}{cm^2K^2}$ for free electrons.[8] This expression in the form of current,

$$I = I_o\left[\exp\left(\frac{qV}{nkT}\right) - 1\right] \qquad 2.9$$

is commonly referred to as the diode equation. The reverse saturation current, I_o, given by

$$I_o = SA^* T^2 \exp\left(-\frac{q\psi_{Bn}}{kT}\right) \qquad 2.10$$

where S is the area of the diode, shows that by operating at lower temperatures, one

would expect the dark current to be reduced. This fact will become very important to the avalanche process in the next chapter.

Other aspects of current transport center on the construction and internal structure of the diode. For example, R. Taylor, et al[10] determined that one could enhance the photoemission process in the detector by constructing thinner metal layers. A possible explanation for this observed enhancement is that if the metal thickness is smaller or comparble to the attenuation length of the hot electrons (or hot holes in p-type semiconductor), reflection or scattering from the metal-ohmic contact interface could redirect electrons over the barrier (see figure 2). In addition, the thinner the metal layer, the less photons will be reflected from the metal-silicon interface, thus improving photoemission.[11] Recent theoretical work has concentrated on explaining photoemission enhancement through collisions with phonons, cold electrons, and scattering from junctions (eg. metal-air, metal-silicon).[12,13]

Thus far we have described the fundamental principles of the Schottky Barrier Diode and discussed the important mathematical expressions that explain the photoelectric characteristics of the diode. In the next chapter the avalanche multiplication process is described.

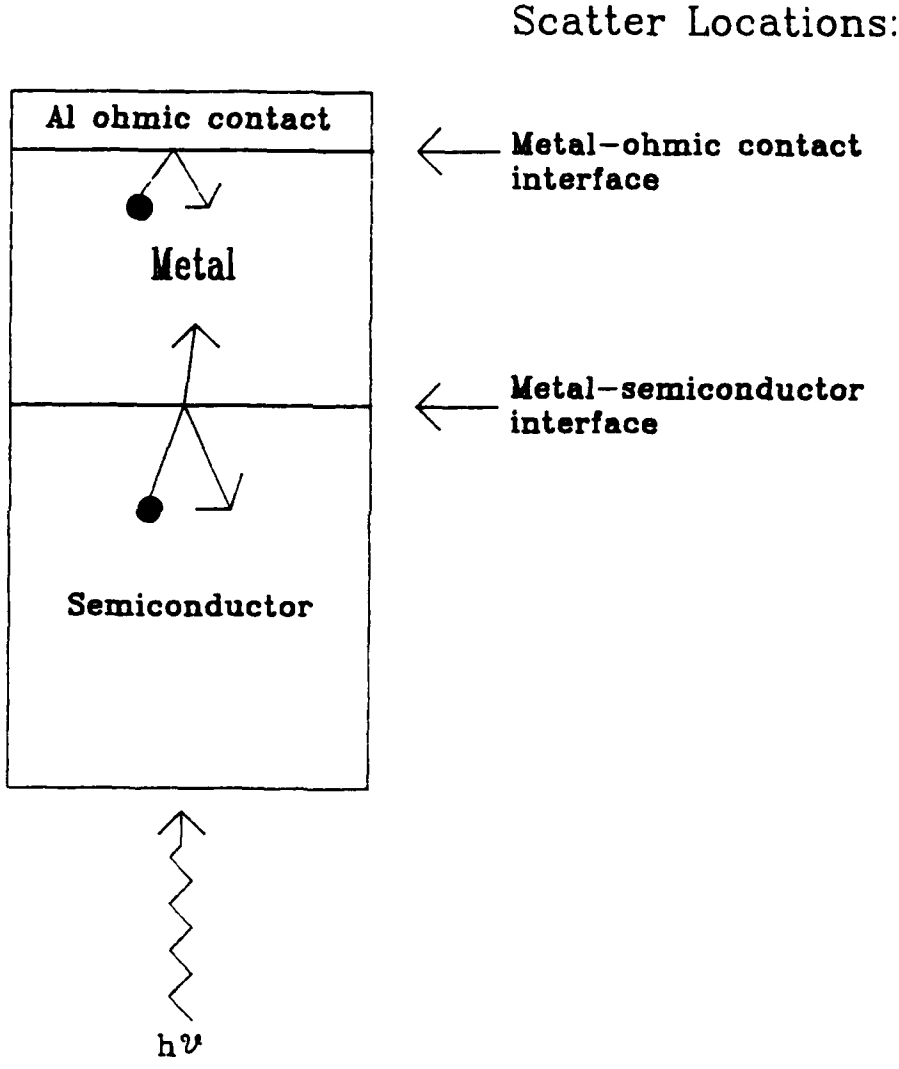

Figure 2. Schottky diode showing interfaces where scattering can occur.

CHAPTER 3

AVALANCHE MULTIPLICATION

Background

The idea of avalanching detectors is certainly not new. The photomultiplier tube and the avalanche photodiode have been around for years. However, the renewed interest in solid state avalanche detectors has been driven by the search for detectors to be used in fiber optic communication systems.[14] The condition under which an avalanche detector is desirable is explained by Webb, et al:[15]

> If amplifier noise is the limiting noise source, it is desirable to have an internal gain mechanism in the detector that multiplies, as noiseless as possible, both the detector signal and detector noise until the latter is greater than the amplifier noise.

The concept is quite simple. If the signal and the noise being detected is below the noise of the amplifier, you multiply that signal and noise until they are greater than the amplifier noise, whereby you are no longer amplifier noise limited. The preceding statement also implies that no advantage is gained by using an avalanche detector if you are noise limited by the signal, background, or dark current.

The discussion on avalanching will be divided into eight parts: 1) signal-to-noise analysis, 2) avalanche gain mechanism, 3) gain-bandwidth product, 4) maximum multiplication, 5) excess-noise factor, 6) linearity and frequency response, 7) examples of avalanche detector structures, and 8) impurity-band conduction.

Signal-to-Noise Analysis

The avalanche process is shown schematically in figure 3. The signal, background, and part of the dark current are all multiplied by the avalanche mechanism. In addition, the schematic shows that excess noise is introduced into the circuit. This is due to the statistical nature of the multiplication process. If we put a signal on the detector described by

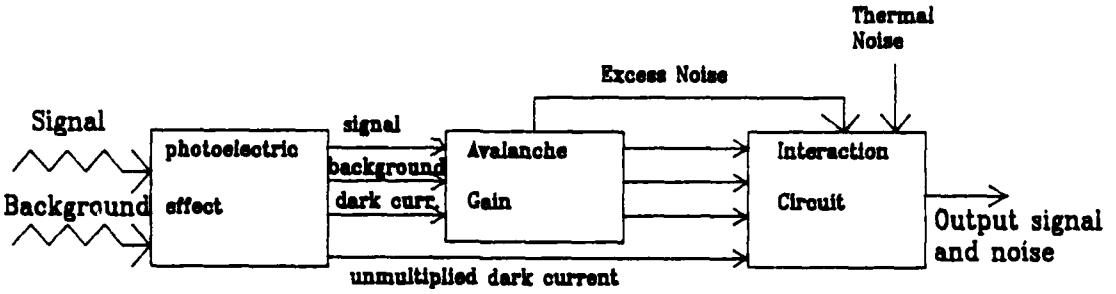

Figure 3. Block diagram showing the avalanche process (after Anderson, et al ref. 28).

$$i_p = \frac{q\eta(\lambda,\omega)\phi_e M(\lambda,\omega)}{h\nu\sqrt{2}} \qquad 3.1$$

where

η = quantum efficiency (wavelength, frequency dependent)

$\frac{\phi_e}{\sqrt{2}}$ = rms incident power (watts)

$M(\lambda,\omega)$ = multiplication (wavelength, frequency dependent)

$h\nu$ = energy of the photon at frequency ν

and we describe the mean square shot noise after multiplication by

$$\langle i^2_s \rangle = 2q[I_p M^2_p F_p + I_B M^2_B F_B + I_{Db} M^2_D F_D + I_{Ds}]B \qquad 3.2$$

where M_P and F_P , M_B and F_B , and M_D and F_D are the average multiplication and excess-noise factor for the average signal, background, and multiplied dark current, respectively, then the signal-to-noise power ratio is

$$\frac{S}{N} = \frac{0.5\left[\frac{q\eta\phi_e}{h\nu}\right]^2 M^2(\lambda,\omega)}{2q[(I_p F_P + I_B F_B + I_D F_D)\, M^2(\lambda,\omega) + I_{Ds}]B + \frac{4kTB}{R_{eq}}} \qquad 3.3$$

where $\frac{4kTB}{R_{eq}}$ is the Johnson noise of the circuit and B is the bandwidth.[14]

All of the dark current is not multiplied when avalanching occurs. Equations 3.2 and 3.3 reflect this statement. The multiplication process occurs in a specific region of the detector, and only the bulk dark current, I_{Db}, is present in this region, and therefore is the component of dark current that is multiplied. The surface leakage current, I_{Ds}, does not undergo multiplication. It is fortunate that I_{Ds} is not multiplied because it can be several orders of magnitude greater than I_{Db}.[14]

If we take equation 3.3 and divide each term by $M^2(\lambda,\omega)$, then

$$\frac{S}{N} = \frac{0.5\left[\frac{q\eta\phi_e}{h\nu}\right]^2}{2q(I_P F_P + I_B F_B + I_{Db} F_D)B + 2qI_{Ds}\frac{B}{M^2(\lambda,\omega)} + \frac{4kTB}{R_{eq}M^2(\lambda,\omega)}} \qquad 3.4$$

and it is easy to see that high multiplication causes the last two terms in the denominator to be insignificant, thereby increasing the signal-to-noise power ratio. The increase will be offset however, by the introduction of excess noise. As will be shown in the section or excess noise, as the multiplication increases, the excess noise will increase (see figure 8). From equation 3.4, an increase in the excess noise will increase the shot noise. Once the multiplication has reduced the importance of the last two terms, further increases in M will cause the increase in the signal-to-noise power ratio to first level off and then decline. Figure 4 shows this result when $F = \sqrt{M}$, the *Johnson noise plus surface dark current squared is* 10^{-12} A^2, and the unmultiplied shot noise squared is 10^{-16} A^2. The optimum multiplication is when the first term in the denominator of equation 3.4 equals the sum of the last two terms in the denominator. From figure 4, for all practical purposes, the optimum multiplication occurs at $M \cong 50$.

For a given desired signal-to-noise and multiplication, the minimum detectable power is given by[14]

$$\phi_e = \frac{2h\nu BF_P}{\eta}\left[\frac{S}{N}\right]\left\{1 + \sqrt{1 + \frac{I_{eq}}{qBF^2P\left[\frac{S}{N}\right]}}\right\} \qquad 3.5$$

where

$$I_{eq} = I_B F_B + D_{Db} F_D + \frac{I_{Ds}}{M^2(\lambda,\omega)} + \frac{2kT}{qR_{eq}M^2(\lambda,\omega)} \qquad 3.6$$

To obtain the signal or quantum noise limit, the background and dark currents must

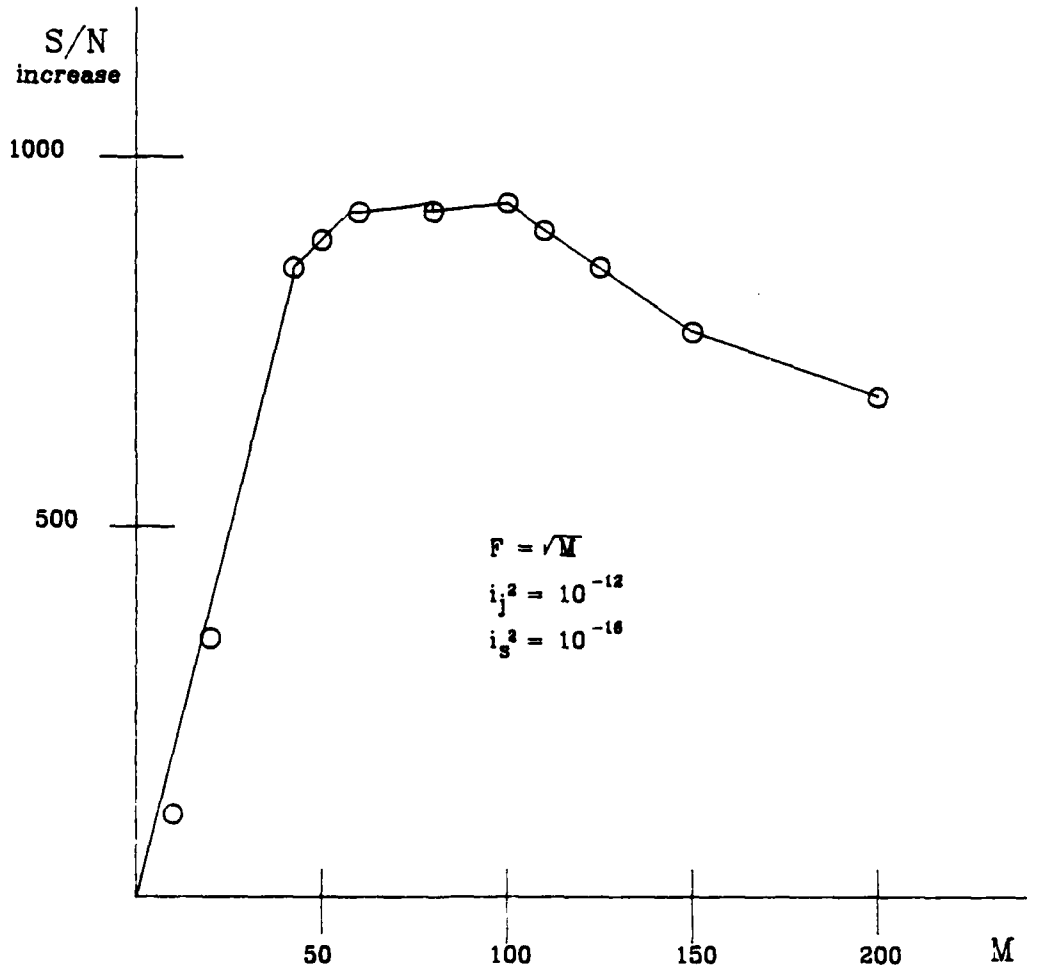

Figure 4. Signal–to noise power increase as a function of multiplication.

be negligible compared to $\frac{2h\nu BF_P}{\eta}\left[\frac{S}{N}\right]$. Therefore multiplication above the pre amp noise in conjunction with low background and dark currents can allow quantum limit performance. Stillman and Wolfe[14] conclude that at high frequencies and large bandwidths, the avalanche detector has an advantage over, for example, a PIN diode because the PIN diode at high frequencies and large bandwidths is limited by thermal noise. This is the type environment one encounters in optical communication systems, making the avalanche diode the ideal candidate. In addition, "the ruggedness, size, speed, and greater quantum efficiency in the near infrared" make solid state avalanche diodes well suited for optical systems.[15]

Avalanche Gain Mechanism

The process by which avalanche gain occurs centers around the concept of impact ionization. By applying a high electric field, primary free carriers (for example those created by incident radiation) collide with valence electrons, creating electron-hole pairs. These additional carriers are also accelerated by the electric field, colliding with other electrons and producing more electron-hole pairs. This process leads to an avalanching effect.

The ionization coefficients are the key parameters in describing how much multiplication can be expected from the avalanching and how the multiplication should be initiated. The coefficients are defined as the "reciprocal of the average distance a carrier will travel at a given electric field before impact ionization generates an additional electron-hole pair."[14] $\alpha(E)$ and $\beta(E)$ are the ionization coefficients for the electron and hole, respectively, in units of cm^{-1}. Stated another way, αdx and βdx are the probabilities that an electron or hole will have an ionizing collision within a distance dx.[15] The ionization coefficients are a function of the electric field, and since the electric field is a function of position in the depletion region, the ionization

coefficients are position dependent. Figure 5 shows the boundary conditions that were used to formulate the expressions for determining multiplication as a function of the ionization coefficients. Stillman and Wolfe [14] show that the multiplication for electrons in terms of α and β is

$$M_n = \frac{\exp\left[\int_0^W (\alpha-\beta)dx\right]}{1-\int_0^W \beta \exp\left[\int_x^W (\alpha-\beta)dx'\right]dx} \qquad 3.7$$

and for holes is

$$M_p = \frac{1}{1-\int_0^W \beta \exp\left[\int_x^W (\alpha-\beta)dx'\right]dx} \qquad 3.8$$

We can look at the importance of α and β on multiplication by examining two special cases. If $\beta = 0$, then $M_p = 0$ and equation 3.7 simplifies to

$$M_n = \exp\int_0^W \alpha dx = \exp \alpha W \qquad 3.9$$

if we assume a constant electric field. The equation shows that finite multiplication will occur as dictated by the value of αW. There is no gain-bandwidth limitation when $\beta = 0$ (or $\alpha = 0$), and the noise due to statistical fluctuations is low because of the large numbers of ionizing carriers present in the depletion region.

In the second case, $\alpha = \beta$. Equations 3.7 and 3.8 simplify to

$$M_p = M_n = \frac{1}{1-\alpha W} \qquad 3.10$$

Avalanche multiplication is infinite when $\alpha W=1$, which corresponds to one ionizing collision per initiating carrier as it transits the depletion region. Although high multiplication can be obtained, the pulse width initiated by the carriers becomes wide, thus

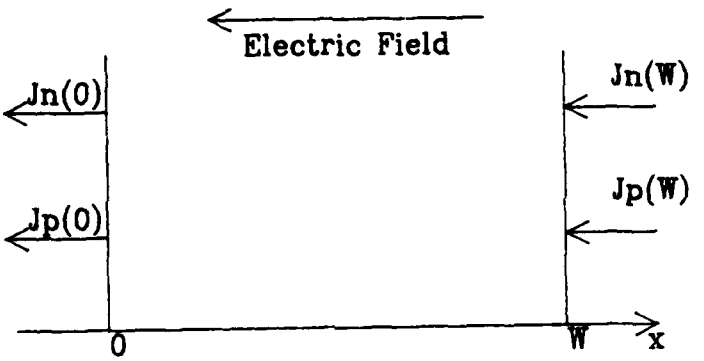

Figure 5. Boundary conditions and electric field direction (after Stillman, Wolfe ref. 14).

imposing a gain-bandwidth product. But most significantly, because of the low number of ionizing carriers in the depletion region, statistical fluxuations will create large amounts of excess noise.[14] Equation 3.10 also shows that when $\alpha=\beta$, there is no preference on which carrier initiates the multiplication.

In the normal situation, α and β will be somewhere between the limiting cases just discussed. If we assume neither α or β are dependent on the position in the depletion region, we can simplify the multiplication equations. For example, equation 3.7 for electron multiplication becomes

$$M_n = \frac{\left[1-\left[\frac{\beta}{\alpha}\right]\right]\exp\left\{\alpha W\left[1-\left[\frac{\beta}{\alpha}\right]\right]\right\}}{1-\left[\frac{\beta}{\alpha}\right]\exp\left\{\alpha W\left[1-\left[\frac{\beta}{\alpha}\right]\right]\right\}} \qquad 3.11$$

Figure 6 shows the gain as a function of αW and the ratio $\frac{\beta}{\alpha} = k$, and the associated electric field required to give αW for a 1μm wide PIN silicon diode. This figure indicates the importance of the ratio $\frac{\beta}{\alpha}$ to the constraints placed on building avalanche detectors. For example, if $\frac{\beta}{\alpha}=1$, slight changes in the electric field will produce large changes in multiplication as indicated by the steepness of the curve. On the other hand, if $\beta\cong 0$, variation in the electric field does not have such a drastic effect on multiplication. The implication is that if you build a detector with materials such that $\frac{\beta}{\alpha}=1$, you are going to have to construct one that has an extremely uniform doping level to avoid unwanted variations in the electric field.[15]

Not only is it important to have materials where α and β are different, one must also initiate the multiplication through carrier injection at the proper point on the detector. Mathematically this is expressed by

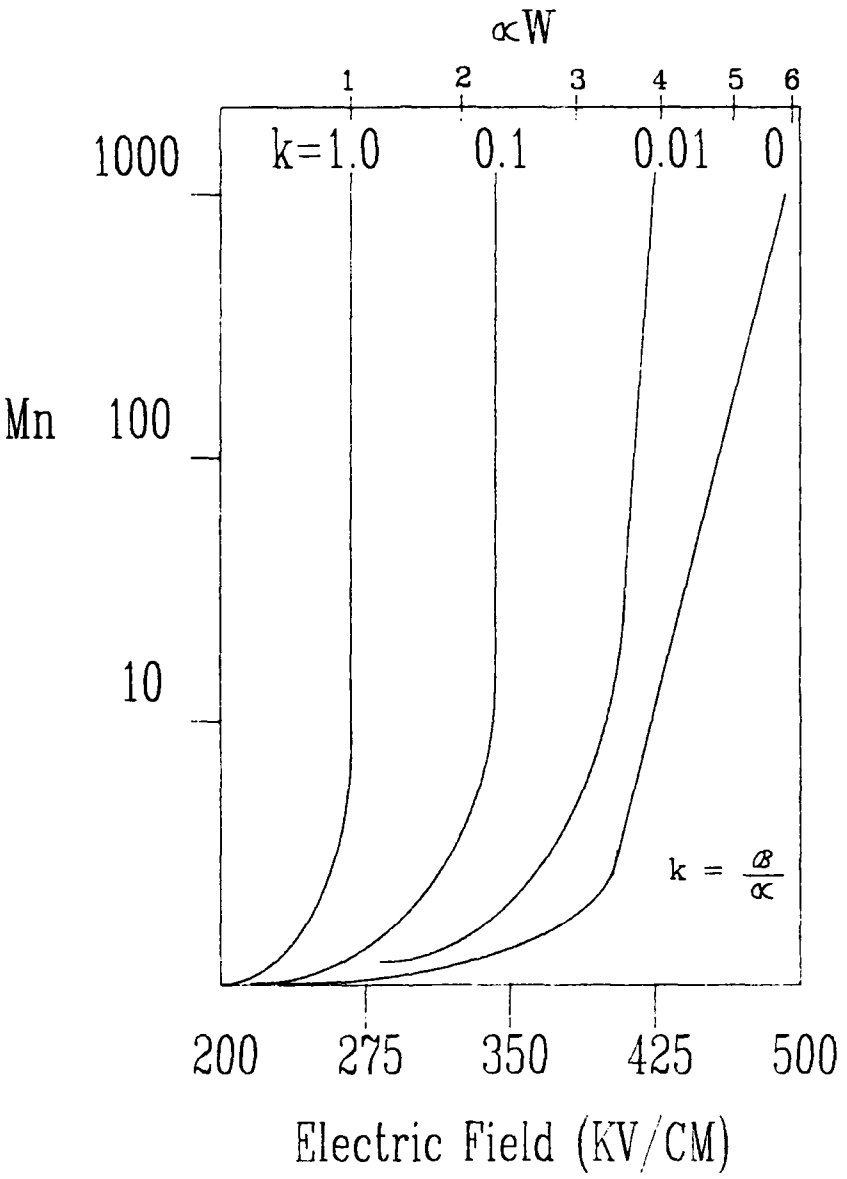

Figure 6. Electron multiplication as a function of electric field with various values of k. (after Webb, et al ref. 15)

$$M(x_o) = \frac{\exp\left[\int_{x_o}^{W} (\alpha-\beta)dx\right]}{1-\int_0^W \beta \exp\left[\int_x^W (\alpha-\beta)dx'\right]dx} \qquad 3.12$$

where equation 3.12 shows that the multiplication is dependent on x_o, the point of injection. Therefore, in a p-n junction, for example, when $\alpha > \beta$, carriers should be injected from the p-side so they can travel the entire depletion region, whereas carriers should be injected from the n-side for $\beta > \alpha$.[14]

Gain-Bandwidth Product

There is a condition under which multiplication is independent of frequency and likewise a condition for which the gain and bandwidth are related. For $\left[\frac{\beta}{\alpha}\right](M_n-1)\ln M_n \leq 1$ multiplication and frequency are independent of one another. For $M_n \geq \frac{\alpha}{\beta}$, the multiplication and frequency are no longer independent and the gain-bandwidth product is given by

$$M(\omega)\omega = \frac{1}{N\left[\frac{W}{v_n}\right]\left[\frac{\beta}{\alpha}\right]} \qquad 3.13$$

where

N= slowly varying number $\left[\frac{1}{3}$ for $\frac{\beta}{\alpha}=1$, 2 for $\frac{\beta}{\alpha}=10^{-3}\right]$

v_n = electron drift velocity

W = width of depletion region

Equation 3.13 shows that for a large gain-bandwidth product, v_n should be large while W and $\frac{\beta}{\alpha}$ should be small.[14] This is the type of conflict one encounters in detectors betweem having W large to maximize quantum efficiency, while at he same time keeping W small to enhance response time.

Maximum Multiplication

Although we have shown mathematically that avalanche multiplication can be infinite, in reality the maximum achievable multiplication is limited by several factors:

1. Voltage drop across the load resistor, across the series resistance of the contacts, and across the undepleted bulk material.
2. Space charge effect in which carriers drifting through the depletion region reduce the electric field.[16]
3. Reduction in the electron and hole ionization coefficients due to junction heating from thermal resistance.
4. Microscopic defects which limit the electric field that can be maintained over the active area.[17]

Melchior and Lynch[18] combined the effects of the first three factors into a differential series resistance R as measured in the breakdown region. They showed that if the dark current was multiplied in the same manner as the photocurrent, the maximum achievable multiplication is given by

$$M_{ph\ max} = \sqrt{\frac{V_B}{nRI_{ph}}} \quad \text{for } I_{ph} >> I_D \tag{3.14}$$

where

V_B = reverse breakdown voltage

R = differential resistance in breakdown region

I_{ph} = photocurrent

I_D = dark current

n = value used to fit equation to experimental data

or $$M_{ph\ max} = \sqrt{\frac{V_B}{nRI_D}} \quad \text{for } I_D >> I_{ph} \tag{3.15}$$

Several very interesting points are derived from these equations. First, a good avalanching detector should have a low differential resistance, which corresponds to a steep I-V curve in the breakdown region (see figure 7). Solder points and electrical connections should be made as clean as possible to avoid unwanted resistance. Second, the dark current must be kept low in order to achieve high multiplication. This may necessitate cryogenic cooling to reduce dark currents. Finally, the detector should have as high a reverse breakdown voltage as possible, tempered by the need to avoid dangerously high voltages and unwanted leakage currents.

The factor n, which should be kept low for high multiplication, is dependent on which carrier initiates the multiplication (which can be dictated by the wavelength of the incident radiation) and the structure and material of the semiconductor. It may seem puzzling that equation 3.14 indicates that as you increase the photocurrent on the detector, the multiplication will diminish. As the photocurrent increases, a greater voltage drop is seen across the series resistance, reducing the voltage drop across the junction, and thus reducing the electric field used for avalanche multiplication.[18]

Excess-Noise Factor

Noise that is generated in a diode occurs because of the random nature of the collection of carriers. If the multiplication process was noiseless, this generated noise would manifest itself as shot noise; that is,

$$\langle i^2_s \rangle = 2qIBM^2 \qquad 3.16$$

However, multiplication is not ideal. The impact ionization must be described statistically and any variation about the average multiplication previously described results in additional noise. Thus the noise portion of equation 3.3,

$$\langle i^2_s \rangle = 2q[(I_P F_P + I_B F_B + I_D F_D) M^2(\lambda,\omega) + I_{Ds}]B + \frac{4kTB}{R_{eq}}$$

shows the introduction of a factor F, called the excess-noise factor. It is defined as

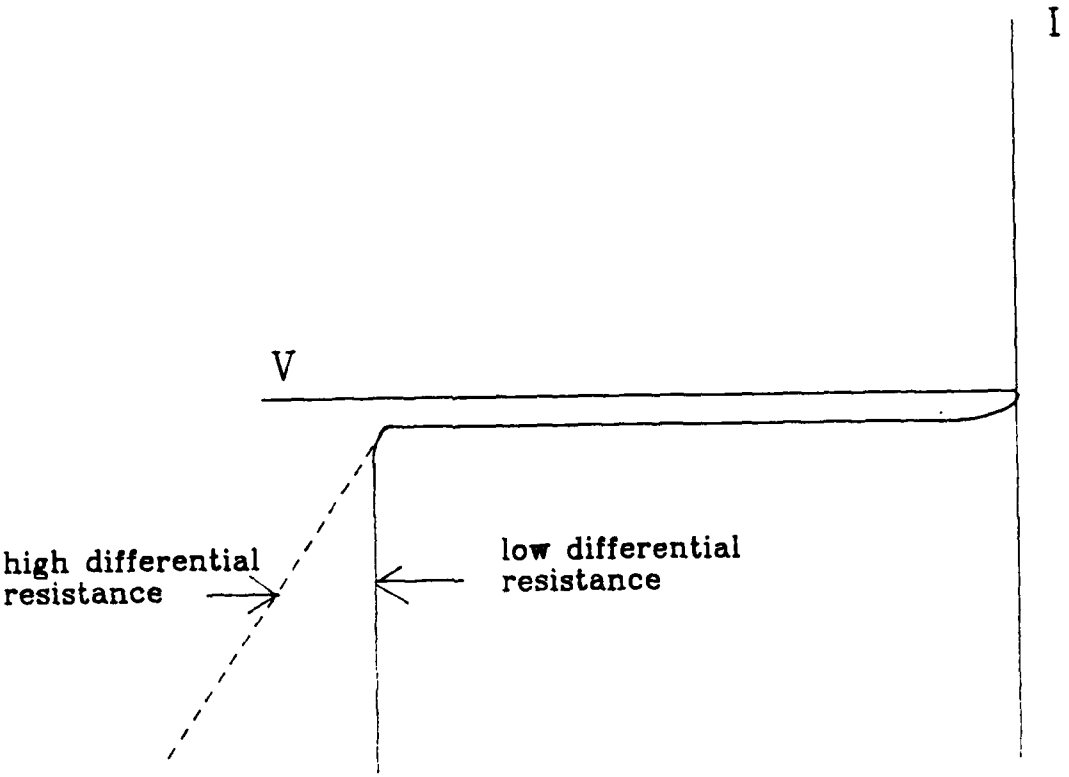

Figure 7. I–V curves showing high versus low differential resistance.

$F = \frac{\langle M^2 \rangle}{\langle M \rangle^2}$, or the variation from the mean value of M. The general expression for F is found by describing the noise spectral density during multiplication. McIntyre[19] derives this expression as

$$\phi = 2q\{2\left[I_n(0)M^2(0) + I_p(W)M^2(W) + \int_0^W gM^2(x)dx\right] + I\left[2\int_0^W \alpha M^2(x)dx - M^2(W)\right]\} \quad 3.17$$

where $I_n(0)$ and $I_p(W)$ are the injected electron (at x=0) and hole (at x=W) carriers, respectively, and g is the photon induced generation rate of electron-hole pairs. When $\alpha=\beta$, equation 3.17 simplifies to

$$\phi = 2qI_t M^3 \quad 3.18$$

where $I_t = I_n(0) + I_p(W) + q\int_0^W g(x)dx$.

Therefore, if we look at equation 3.16, $\frac{\langle i_s^2 \rangle}{B} = 2qIM^2$, we can see that the excess noise introduced when $\alpha=\beta$ is M, so that

$$\frac{\langle i_s^2 \rangle}{B} = 2qI_t M^2 F \text{ where } F=M.$$

If $\beta=k\alpha$ is a constant, then the excess-noise factor is different for pure electron and hole injection, and is given by[14]

$$F_n = M_n\left\{1-(1-k)\left[\frac{M_n - 1}{M_n}\right]^2\right\} \quad 3.19$$

$$F_p = M_p\left\{1-\left[1-\left(\frac{1}{k}\right)\right]\left[\frac{M_p - 1}{M_p}\right]^2\right\} \quad 3.20$$

Figure 8 shows plots of F_n or F_p versus multiplication at various values of k. This graph supports the idea that detectors should be constructed of materials where α and

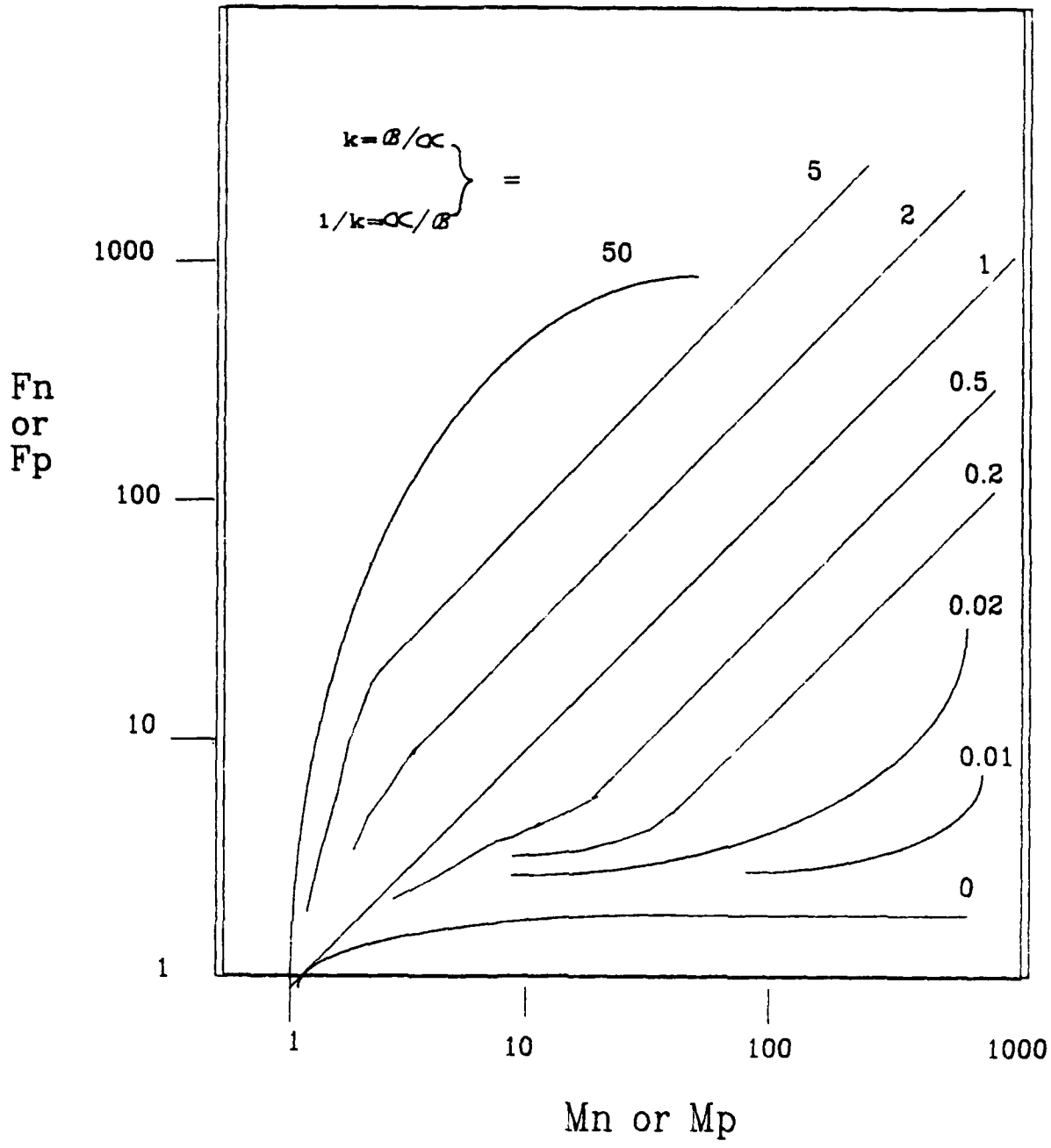

Figure 8. Excess-noise factor versus multiplication (after Stillman, Wolfe ref. 14).

β differ greatly. Thus, we see that for pure electron injection, $k=\frac{\beta}{\alpha}$ must be small, and for pure hole injection, $\frac{1}{k} = \frac{\alpha}{\beta}$ must be small, and this will keep the excess-noise factor low.

We can analyze equation 3.19 by once again looking at two limiting cases: $\beta=0$ and $\alpha=\beta$. By setting k=0 in equation 3.19, we get

$$F_n = M_n\left\{1-\left[\frac{M_n - 1}{M_n}\right]^2\right\}$$

$$\cong 2 \text{ for } \frac{1}{M^2_n} << \frac{2}{M_n} .$$

Therefore, if $\beta\cong 0$ (k=0), the excess noise factor would be 2. This would be our lowest attainable excess-noise factor. For $\alpha=\beta$ (k=1), $F_n = M_n$, as previously shown.

If the injected carrier is a mix of electrons and holes, then F is given by[15]

$$F_{eff} = \frac{fM^2_n F_n + (1-f)M^2_p F_p}{[fM_n + (1-f)M_p]^2} \qquad 3.21$$

where $f=\frac{I_n(0)}{[I_n(0) + I_p(W)]}$ is the ratio of electron to total injected current. Figure 9 shows how the excess-noise factor varies with multiplication for a fixed value of k and various values of f. This graph shows that not only is it important to have small values of k, you must also initiate avalanching with the carrier that has the higher ionization coefficient. Thus, at k= 0.005 you get the lowest excess-noise factor when f=1, or pure electron injection.

Linearity and Frequency Response

The linearity of avalanche detectors as reported by Webb[15] covers several orders of magnitude, from 10^{-14} watts to 10^{-8} watts. The high end of the incident power range is limited by gain saturation effects previously described under the section on maximum achievable multiplication.

The frequency response is affected by the transit-time of the carriers and also by the time it takes for avalanche multiplication to occur. This was briefly described

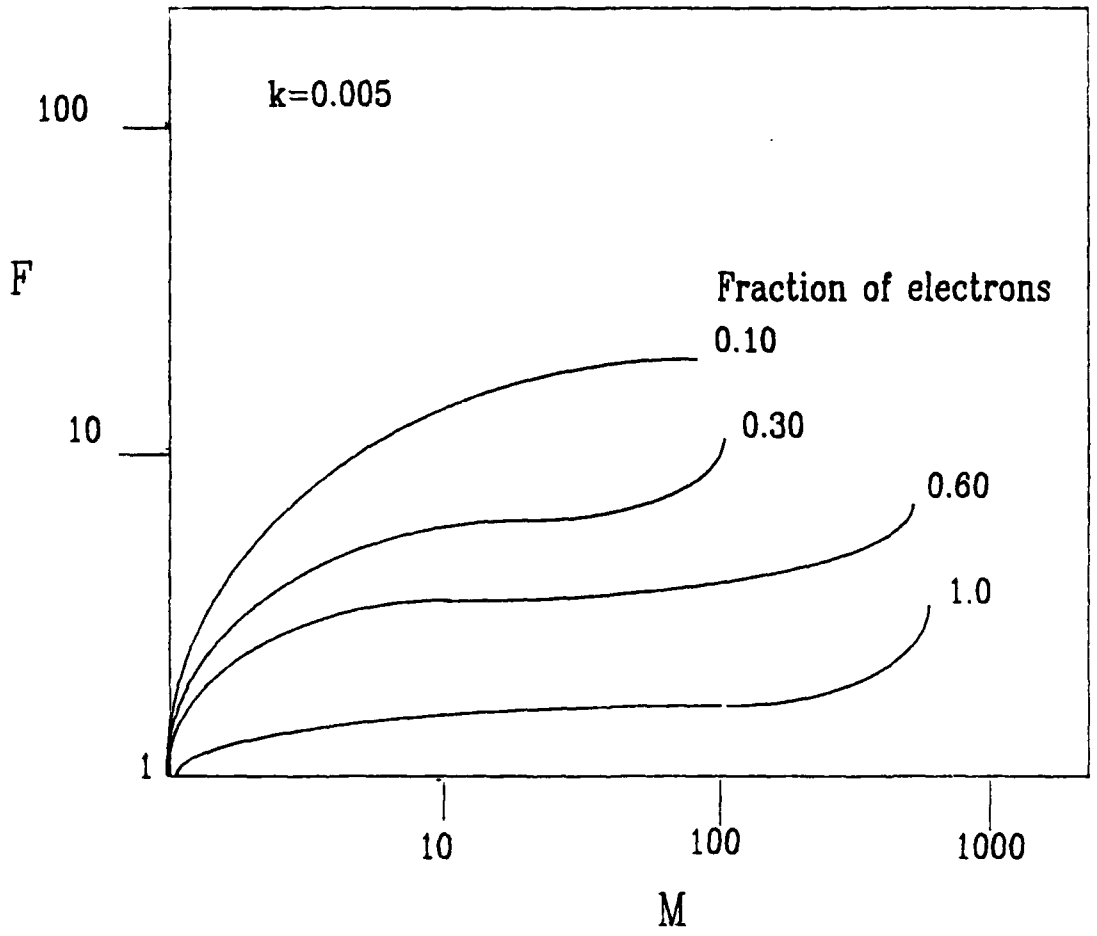

Figure 9. Excess–noise factor versus multiplication for various fractions of injected electrons (after Webb, et al ref. 15).

earlier as contributing to a gain-bandwidth product limitation. Webb shows that for transit-time effects,

$$M(\omega) = \frac{M(0)\exp\left\{-\frac{j\omega M(0)\tau_m}{2}\right\}}{1 + j\omega\tau_m M(0)} \qquad 3.22$$

while the frequency dependance of multiplication time can be described by

$$M(\omega) = \frac{M(0)}{1 + j\omega\tau_m M(0)} \qquad 3.23$$

where M(0) is multiplication at low frequency, and τ_m is the effective multiplication time which is primarily dependent on the device structure. As an example, Webb states that τ_m is typically less than a picosecond and therefore $M(\omega) = M(0)$ up to about 200 GHz.[15]

Examples of Avalanche Detector Structures

Although this work is investigating the use of PtSi SBD's as avalanche detectors, it is beneficial to briefly discuss some of the other structures and materials being investigated by the detector community. Detectors constructed with a P-I-N junction have been used to study ionization coefficients of materials because the electric field is constant across the depletion region (thus simplifying mathematical expressions) and also pure electron or hole injection can be accomplished by selecting the proper side for irradiation. However, their use as avalanche detectors is not widely reported in litura-ture. Detectors fabricated with P-N junctions are used as avalanche detectors, although their mathematical descriptions are more complicated due to their electric field dependence on position. Silicon and germanium were the early materials investigated as avalanche detectors. Other developments include the use of InAs and InSb as avalanche detectors[14] and more recently the investigation by the Air Force of GaAlSb as an avalanche detector.[20]

Another structure investigated is the Reachthrough Avalanche Photodiode (RAPD). This device allows a wider depletion region while at the same time lower breakdown voltage. The wider depletion region enhances the long wavelength quantum efficiency and the lower breakdown voltage helps reduce leakage currents from edge effects. An example is the Ge RAPD which uses a P^+-N-N^- structure.

Recent investigations have centered on developing long wavelength detectors that use separate absorption and multiplication (SAM) layers, thus reducing the leakage current, and finally superlattice structures that use layers of continuously graded bandgap materials to artificially increase the ionization coefficient ratio and thereby reduce noise.[1]

The Schottky diode has two features that make it ideal for use as an avalanche detector: 1) single carrier injection and 2) spatial localization. The most attractive feature is that SBD's allow pure electron or pure hole initiation in the same diode simply by wavelength selection of the incident radiation. In 1973 Woods, et al used the Schottky diode to measure the ionization coefficients in silicon because of this pure injection feature. Figure 10 shows how one can obtain separate electron and hole injection in the diode. If you backside illuminate the diode with energy $h\nu$ greater than the barrier height but less than the bandgap energy ($\psi<h\nu<E_g$), the photons will pass through the semiconductor and cause internal photoemission in the metal, and as discussed in chapter 2, electrons with energy greater than the barrier height will pass over the barrier into the semiconductor. One therefore gets "pure electron injection". On the other hand, if $h\nu$ is greater than the semiconductor bandgap ($h\nu>E_g$), the photon is absorbed in the semiconductor and the normal electron-hole pair is created, with the holes diffusing towards the depletion region. Thus one can get "pure hole injection".[21]

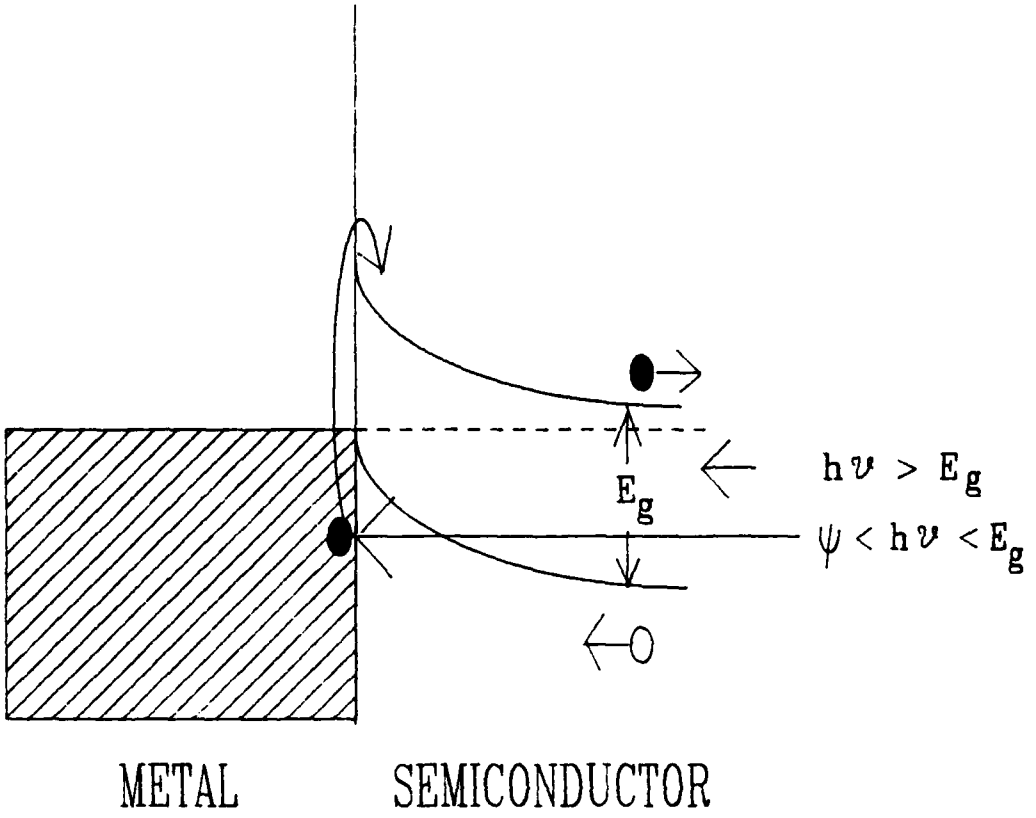

Figure 10. Energy diagram showing separate electron and hole injection by selection of wavelength (after Woods, et al ref. 21).

The ability to select the carrier for impact ionization becomes very convenient for our use of PtSi diodes. Since the ionization coefficient for electrons, α, is greater than that for holes, β, in silicon, the avalanche process should be initiated by using electrons. This means using photons with energy $\psi < h\nu < E_g$. As will be shown in the results section, this wavelength selection allows us to detect photons between 1.1 and 1.5 microns, covering our stated region of interest for fiber optic systems. Therefore, by using PtSi SBD's, we have a detector which has a photoresponse in the required wavelength region, while at the same time is constructed of materials such that at these wavelengths, the avalanche process is maximized and the excess noise introduced by multiplication is minimized.

Impurity Band Conduction

The discussion to this point on avalanching has been based on valence-to-conduction band impact ionization. Recent works have investigated impact ionization based on impurity-band conduction.[22] Figure 11 shows the process for an n-type semiconductor. This theory is based on conduction occurring between the impurity level and the conduction band. The process is due to quantum effects that are present at high impurity concentrations ($N_D = 10^{17}$ cm^{-3}) and low temperatures ($T \cong 10^{\circ}$K). Petroff, et al[23] describe an arsenic doped silicon (Si:As) detector used for counting photons in the wavelength range from 0.4 to 28 μm. They show high multiplication at low reverse bias ($V \cong 5$ volts). Multiplication at low reverse bias indicates impurity-band impact ionization occurs at much lower electric field strengths than is required to produce valence-to-conduction band impact ionization. This is so because the ionization energy for impurities in silicon is $\cong 0.025$ eV[8] whereas valence-to-conduction band ionization energy for silicon is $\cong 8$ eV[24] . When the electron-hole pair is created by impurity-band ionization, the electron experiences high drift velocities towards the

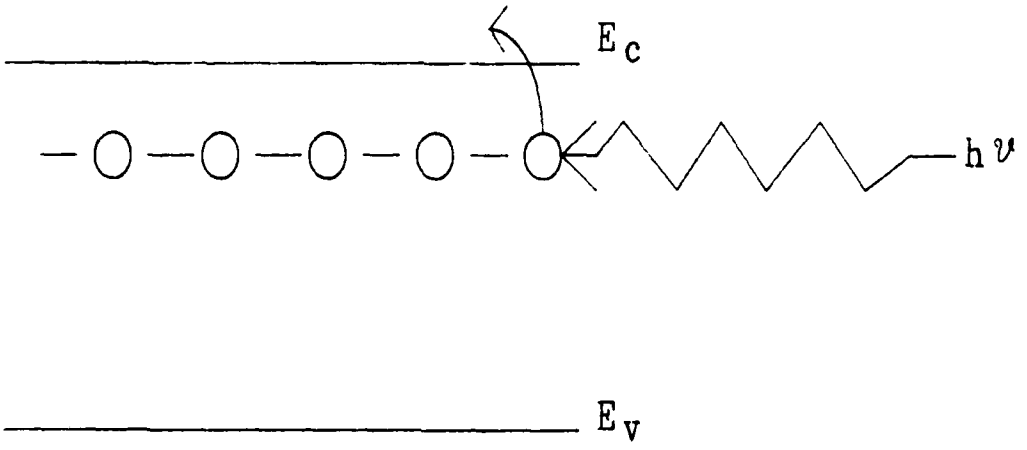

n-type semiconductor

$N_D = 10^{17} cm^{-3}$

T = 10 K

Figure 11. Impurity-band impact ionization process.

multiplication region, while the hole drifts slowly in the opposite direction. This will result in nearly noise-free gain.

Capasso, et al[25] described the ionization across band discontinuities of carriers confined in quantum wells of superlattice structures. Hot electrons in the barrier layers collide with bound electrons in the wells causing impact ionization. Once again, multiplication occurs at low electric fields as compared to valence-to-conduction band ionization. Other interesting results from their investigation showed that as the dark current increased, the onset of multiplication occured at lower reverse bias, and the same result was seen as the temperature was increased from 70 to 300°K. The key benefit of producing avalanching using impurity-band ionization is that gain occurs at low reverse bias, which is good for safety reasons as well as reducing edge and leakage currents that are present at high reverse bias. Thus, one can expect nearly noise-free avalanching.

CHAPTER 4

EXPERIMENTAL ARRANGEMENTS FOR PtSi INVESTIGATION

Platinum Silicide Diodes

The Schottky Barrier Diodes analyzed for this work were provided by the Rome Air Development Center (RADC), Hanscom AFB, Mass. The diodes were constructed by depositing 20 angstroms of Pt on an n-type Si substrate. The bulk resistivity of the Si substrate is 5 Ω-cm nominal, corresponding to a donor concentration of 10^{15} cm^{-3} . The diodes were then annealed in forming gas at 350 degrees C, and this causes the Pt layer to change sequentially from Pt-Si to Pt-Pt_2Si-Si, Pt-Pt_2Si-PtSi-Si, and Pt_2Si-PtSi-Si into PtSi-Si as the annealing temperature or time are varied. The detectors for this study were annealed until the final stage of PtSi-Si was reached. The final steps included the construction of a guard ring by p-type ion implantation to reduce the edge and leakage currents, and the evaporation of 3000 angstrom thick aluminum to provide ohmic electrical contacts to the anode and cathode. Figure 12 shows a diagram of the diodes, where four individual diodes are constructed on a chip approximately 5 mm by 5 mm in dimension. The unpackaged diodes were then analyzed on a I-V curve tracer, using probes to make electrical contact, in order to select diodes with good I-V characteristics such as low reverse saturation currents and sharply defined breakdown points. Once a chip was selected that had good diodes, it was mounted on a TO-5 transistor header or an IC dip package, which had a hole drilled in the center to allow for backside illumination. Wire bonding was then performed to make electrical connections for the anode and cathode. In order to analyze the diodes at cryogenic temperature, the TO-5 header was mounted in a dewar and cooled with liquid nitrogen. The temperature was monitored using a calibrated IN 914 diode mounted with the TO-5 header.

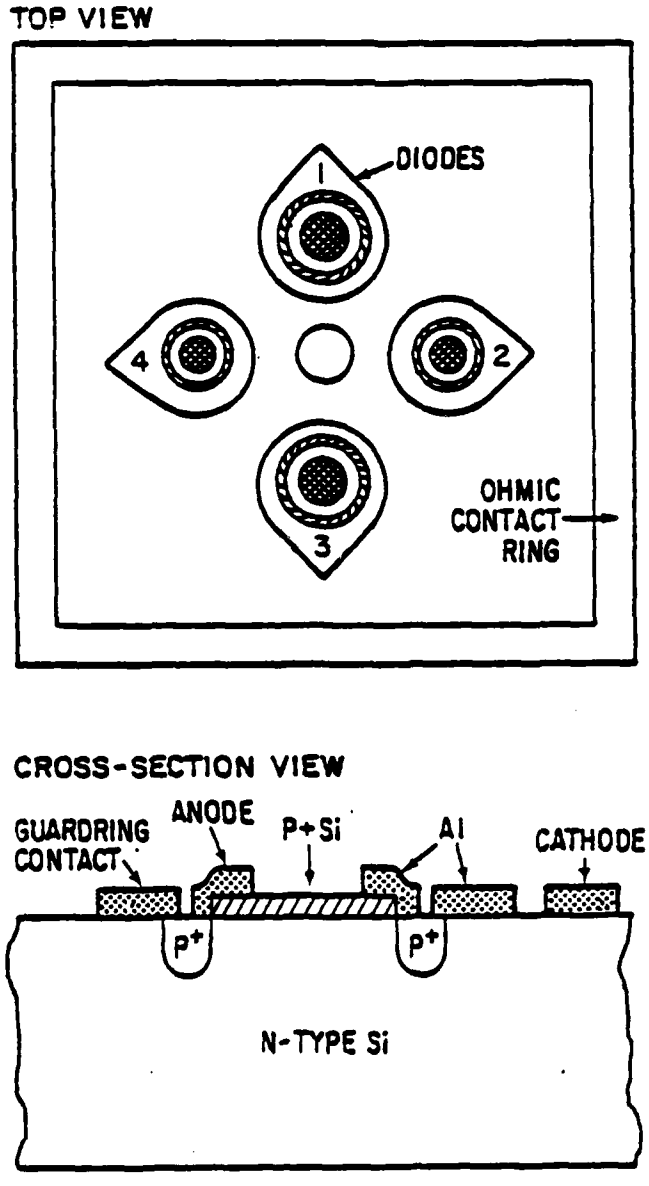

Figure 12. Top and crossectional views of PtSi diode supplied by Hanscom AFB (RADC).

Measurements Performed

In an effort to analyze the compatibility of the PtSi diodes for use as an avalanche detector in optical communication systems, several parameters were measured to help quantitize the diode's performance. These measurements included forward and reverse dark currents, ideality factor, Schottky barrier height, spectral response, quantum efficiency, reverse breakdown voltage, and finally the avalanche multiplication and excess-noise characteristics.

The I-V characteristics of the diodes were measured to determine the amount of dark current at room temperature as well as 85° K. Figure 13 shows the transimpedance amplifier circuit used to measure the diode current in the reverse bias mode. The circuit was calibrated using a Kethley picoamp source and verified with a Kethley electrometer. By manually stepping through increments of voltage, the current was read at each step, and thus an I-V curve was generated.

The forward current was measured to determine the ideality factor, n, found in the diode equation, $I=\left[\exp \frac{qv}{nkT} - 1\right]$. Solving for n,

$$n= \frac{q}{kT} \left[\frac{\partial \ln I}{\partial V}\right]^{-1} \qquad 4.1$$

For a given temperature, a plot of lnI versus V will give the value of the inverse slope needed to calculate n. Diodes that follow the characteristics of the diode equation are considered good if n is between one and two.

The Schottky barrier height determines the long wavelength cutoff of the detector, and thus its value is important in determining the spectral response. There are several techniques that can be used to measure the barrier height. The photoelectric technique was used in this study. This technique is based on the Fowler expression for photoyield as a function of photon energy,

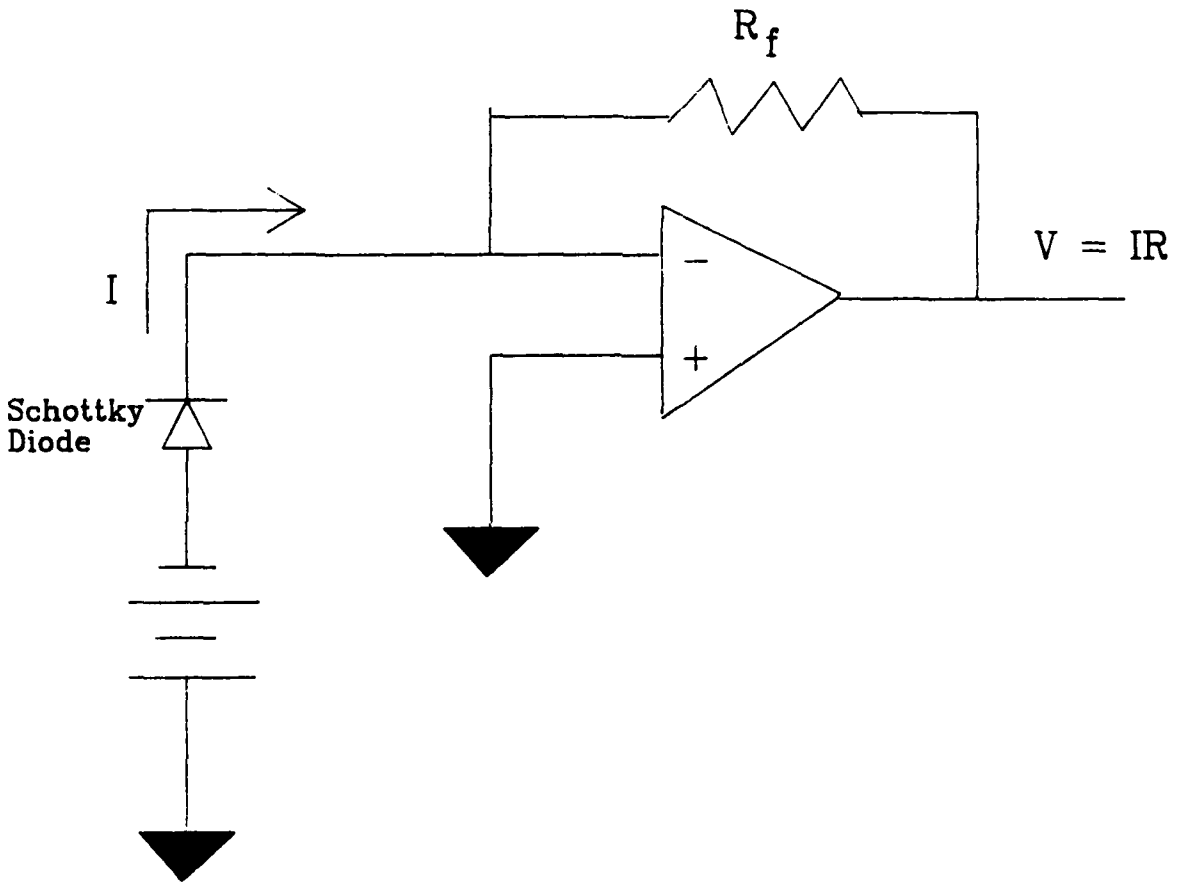

Figure 13. Transimpedance amplifier circuit with reverse bias for detector readout.

$$Y = \frac{C1(h\nu - \psi)}{h\nu} \qquad 4.2$$

where C1 is a constant.[26] By plotting $\sqrt{Yh\nu} = \sqrt{R(\lambda)}h\nu$ versus photon energy (eV), where $R(\lambda)$ is the responsivity in $\frac{amps}{watts}$, a Fowler plot is generated, and by extrapolating the linear portion of the curve to where it crosses the energy axis, the barrier height can be read directly from the graph.

The spectral response of the PtSi diodes was measured, with particular attention directed at the 1.3 μm to 1.6 μm region. The task was accomplished using a Perkin Elmer model 98 monochrometer with a calcium floride prism for near infrared wavelength selection. A tungsten-halogen lamp was used as the source. An absolute calibration was made on the source using a thermocouple detector whose responsivity was measured on a blackbody. A thermocouple was used because of its flat response over a large spectral band. The detector was masked to match the diameter of the active diode area. Figure 14 shows a plot of the power on the detector as a function of wavelength. Once the calibration was accomplished, the thermocouple was replaced with the PtSi diodes and their responsivity measured.

Closely associated with the spectral response is the quantum efficiency as a function of wavelength. By knowing the power, ϕ_e, incident on the detector and measuring the detector signal current, I_s, one can calculate the quantum efficiency as a function of wavelength by

$$\eta = \frac{\frac{I_s}{q}}{\frac{\phi_e \lambda}{hc}} \qquad 4.3$$

The data for the incident power as a function of wavelength is taken from figure 12.

Finally, the multiplication and excess noise introduced by avalanching will be analyzed. Multiplication of the photocurrent can be analyzed by chopping the signal at 100 Hz and looking at the output on a HP Wave Analyzer. Figure 15 shows the

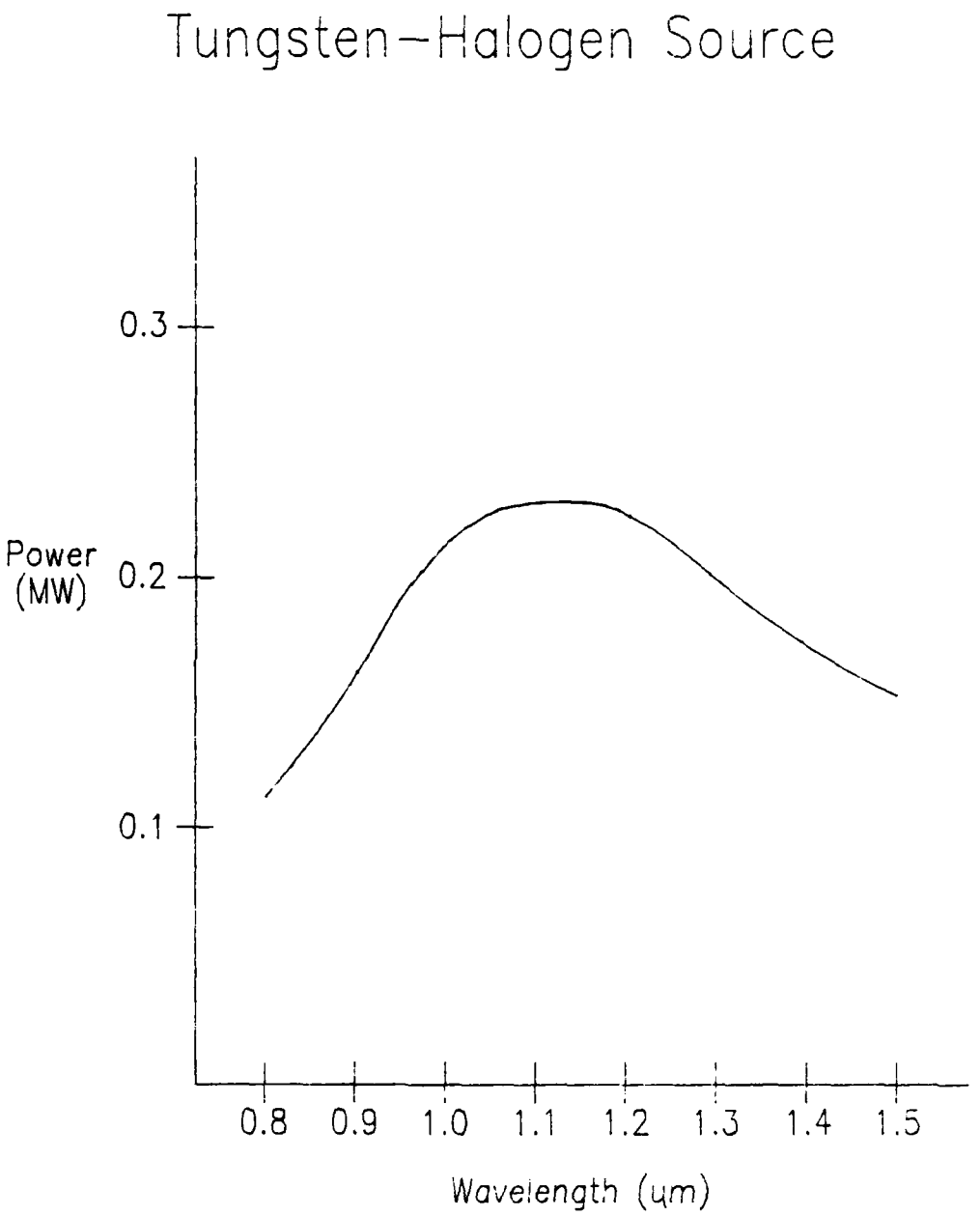

Figure 14. Power incident on detector versus wavelength.

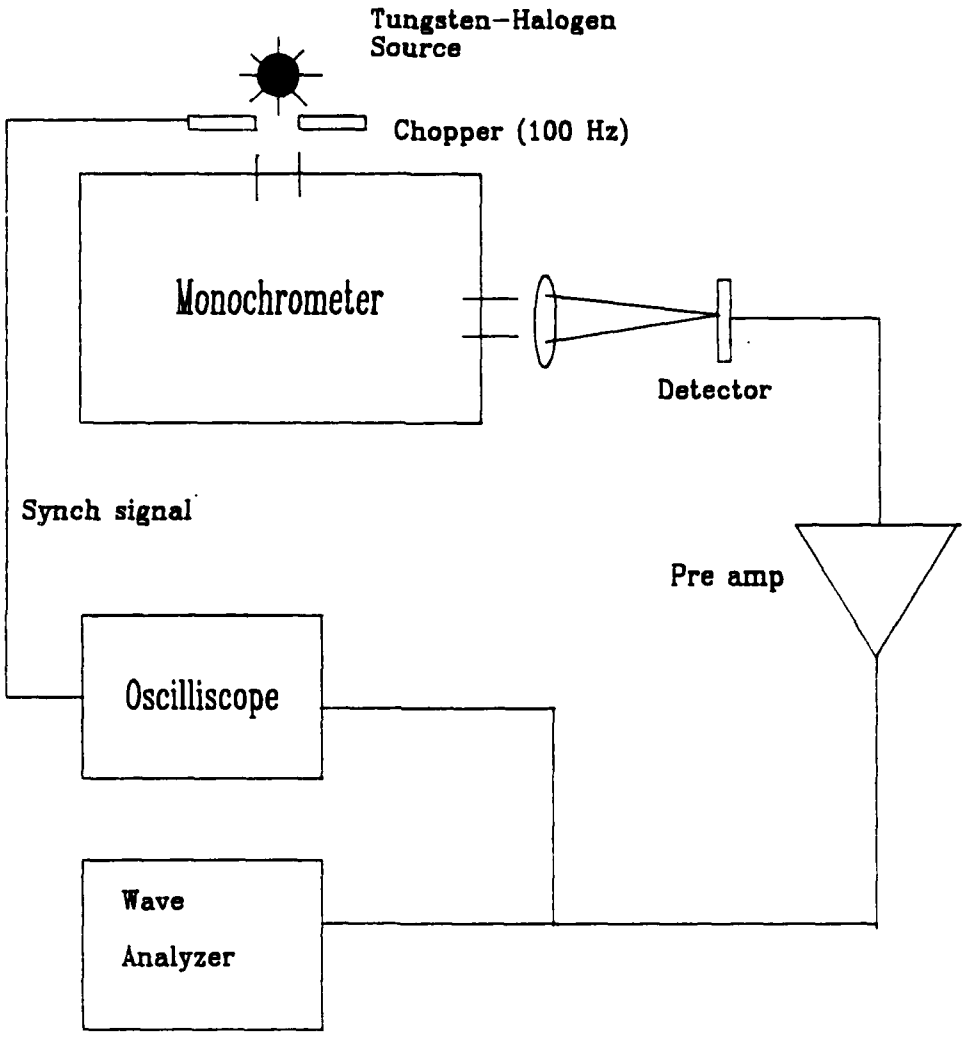

Figure 15. Test set up for measuring responsivity and multiplication.

schematic setup of the test. The signal, V_s, is measured in the non-multiplying region (ie. low reverse bias) and then measured in the multiplying region at reverse breakdown, V_{sb}. Then $M = \frac{V_{sb}}{V_s}$. The noise is then analyzed to see what additional noise is introduced by multiplication. As the reverse bias is increased and the dark current increases, an increase in shot noise will occur according to $2qI_dB$. Any additional noise measured above shot noise can be attributed to the multiplication process and the excess-noise factor ($2qI_dFB$). If the excess-noise factor is not kept as small as possible, the signal-to-noise ratio will decrease during the multiplication process.

CHAPTER 5

EXPERIMENTAL RESULTS

Initial measurements were made on a I-V curve tracer to select diodes with good I-V characteristics. Figure 16 shows some examples of these curves for different diodes. The data shows the diode characteristics can vary quite markedly, even when the diodes are on the same wafer, as in the case of 16a and 16b. The diodes in 16b and 16c actually have more ohmic than diode characteristics. Previous analysis performed on other diodes provided by RADC indicated that deterioration and difficulty in making good electrical contact with probes or wire bonds may contribute to poor diode characteristics.[26] Another possibility may be inhomogenities in the donor concentration of the silicon, producing ohmic characteristics as the donor concentration becomes greater than 10^{15} cm^{-3} . Figure 16 also shows that diodes exhibit reverse breakdown between 6 and 14 volts at room temperature. Diodes 16a, e, and f were selected for further analysis. A more precise I-V curve was then generated to look at the dark currents. Figure 17 shows the dark currents of the three diodes at room temperature. At one volt reverse bias, the dark current is approximately one microamp for diodes 16a and 16f, and an order of magnitude lower for diode 16e. Unfortunately, these levels of dark current at room temperature, coupled with a measured differential resistance on the order of 10kΩ, will limit the maximum multiplication we can expect to see at room temperature according to equation 3.14,

$$M_{ph\ max} = \sqrt{\frac{V_B}{nRI_d}}$$

so that with V_B = 14 volts, n = 5, R = 10KΩ, and I_d = 1μA, the expected maximum multiplication would be ≅ 16. To examine the dark current at cryogenically cooled temperature, diode 14f was mounted in a dewar, evacuated to 5 x 10^{-5} mm Hg, and

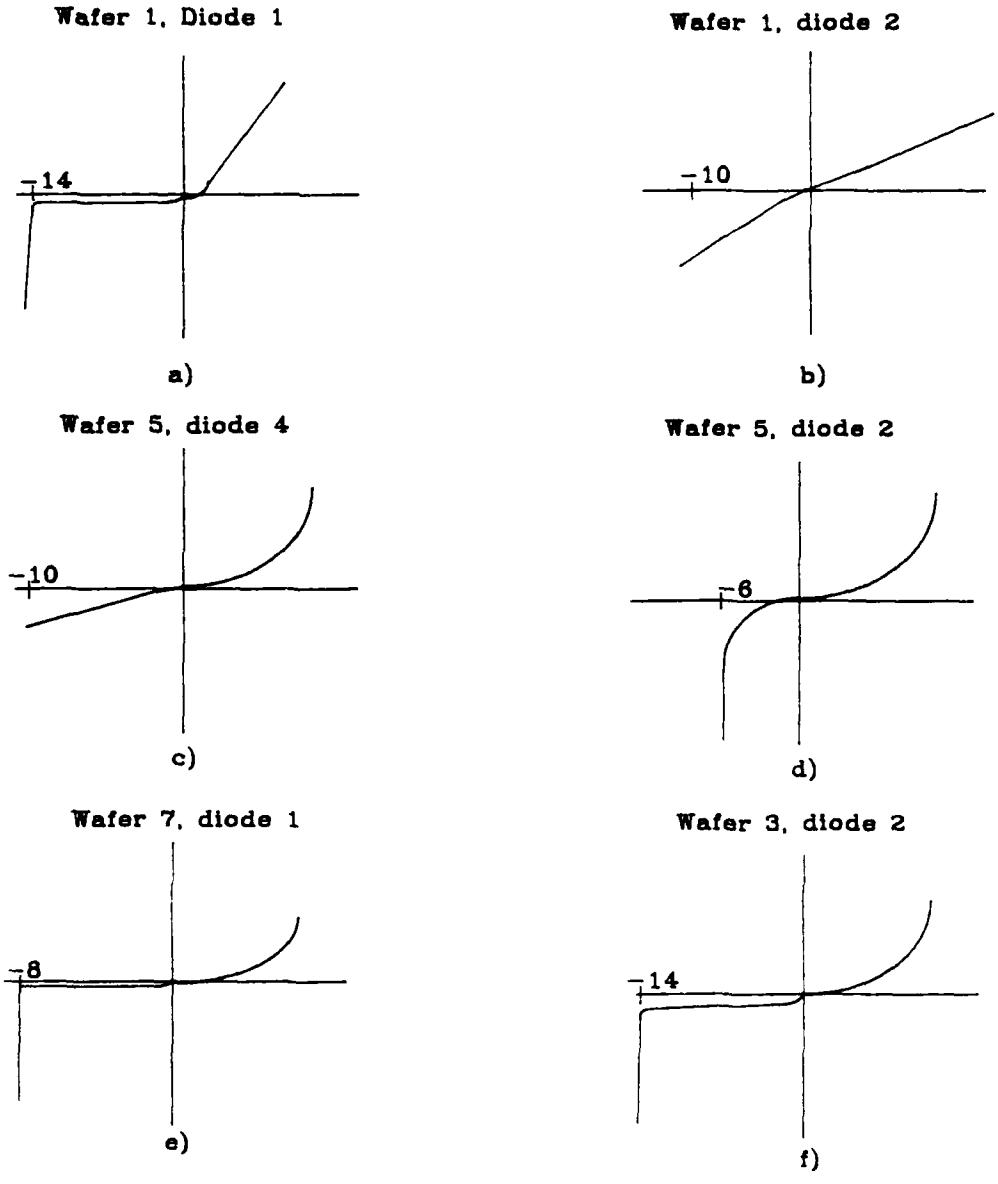

Figure 16. I–V curves for various PtSi diodes.

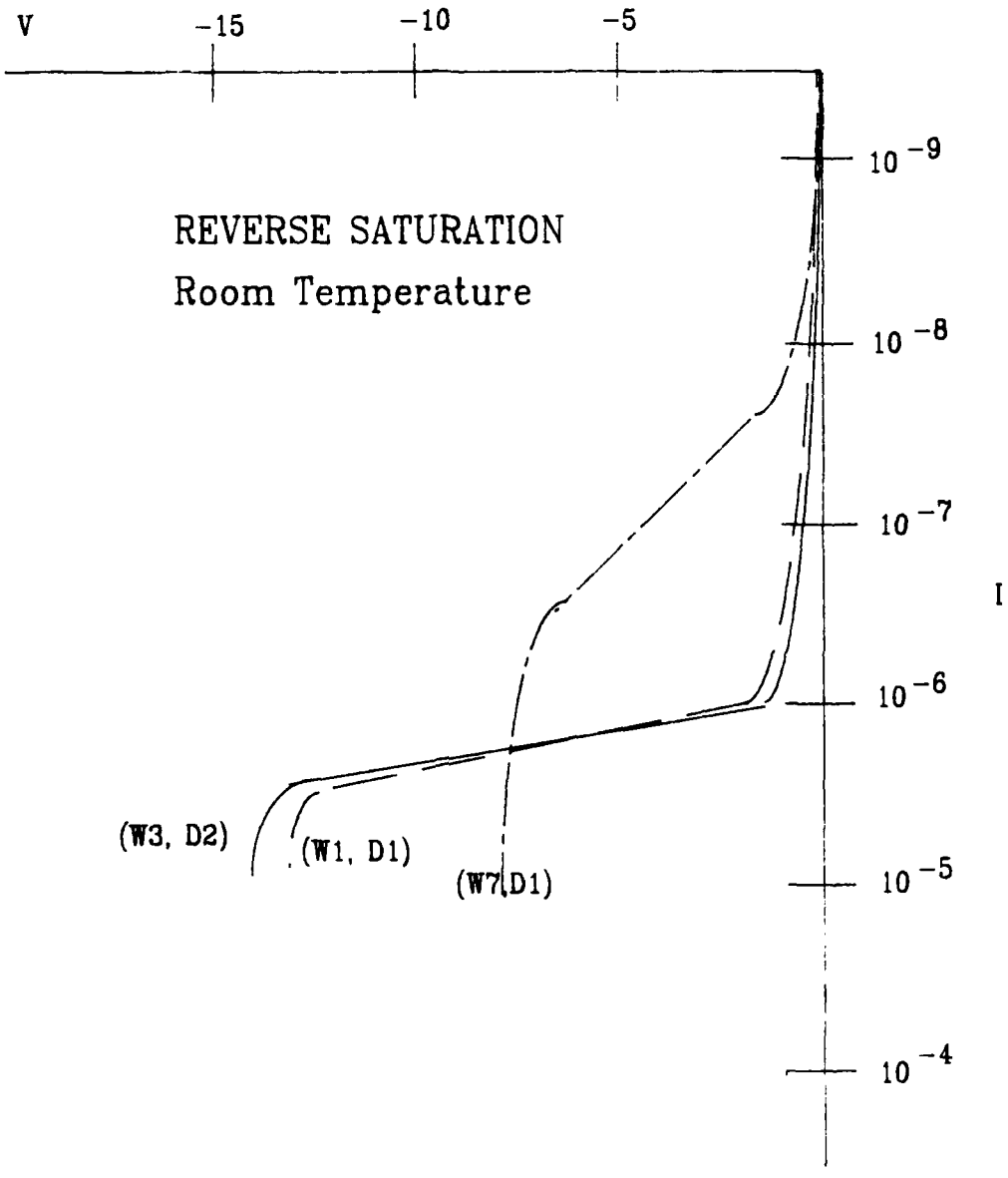

Figure 17. Reverse saturation current for diodes a,e, and f (ref. figure 16).

cooled to 85° K with liquid nitrogen. Figure 18 shows the dark current at T=85° K as well as room temperature for comparison. The dark current has been reduced by three orders of magnitude. The lower dark current will reduce the associated shot noise and therefore increase the signal-to-noise ratio, or for a given signal-to-noise decrease the minimum detectable power (see equation 3.5). The maximum achievable multiplication for photocurrent would increase to ≅ 530.

The forward currents for diodes 16e and 16f were measured in order to calculate the ideality factor n, using equation 4.1. Diode 16e had an ideality factor of 2.53 and diode 16f had a value of 3.06. Both values are higher than what is normally considered good, indicating a departure from the diode equation. It is thought that this departure from the ideal is due to an increase in the contact resistance as the forward bias increases, resulting in higher calculated values of n.[26]

Figure 19 shows the results for the Schottky barrier height measurements using the photoelectric technique. The extrapolated curve crosses the energy axis at 0.92 eV. This value is higher than barrier heights for PtSi-Si given in literature (0.85 eV). If the long wavelength cutoff is determined by equation 2.3,

$$\lambda_{max} = \frac{1.24}{\psi}$$

then we can estimate that our cutoff wavelength would be near 1.35 microns.

The responsivity, R(λ), and the quantum efficiency, η, were measured as a function of wavelength in order to characterize the spectral response of the detector. The reverse bias was one volt. As figure 20 shows, the long wavelength cutoff occurs between 1.4 and 1.5 microns (slightly longer than predicted by the barrier height measurement), with the peak responsivity and quantum efficiency occuring at 1.05 microns. At 1.3 microns, the quantum efficiency is approximately 0.01 percent. This would seem to pose a problem for our detection of energy in the 1.3 to 1.5 micron

WAFER 3, DIODE 2

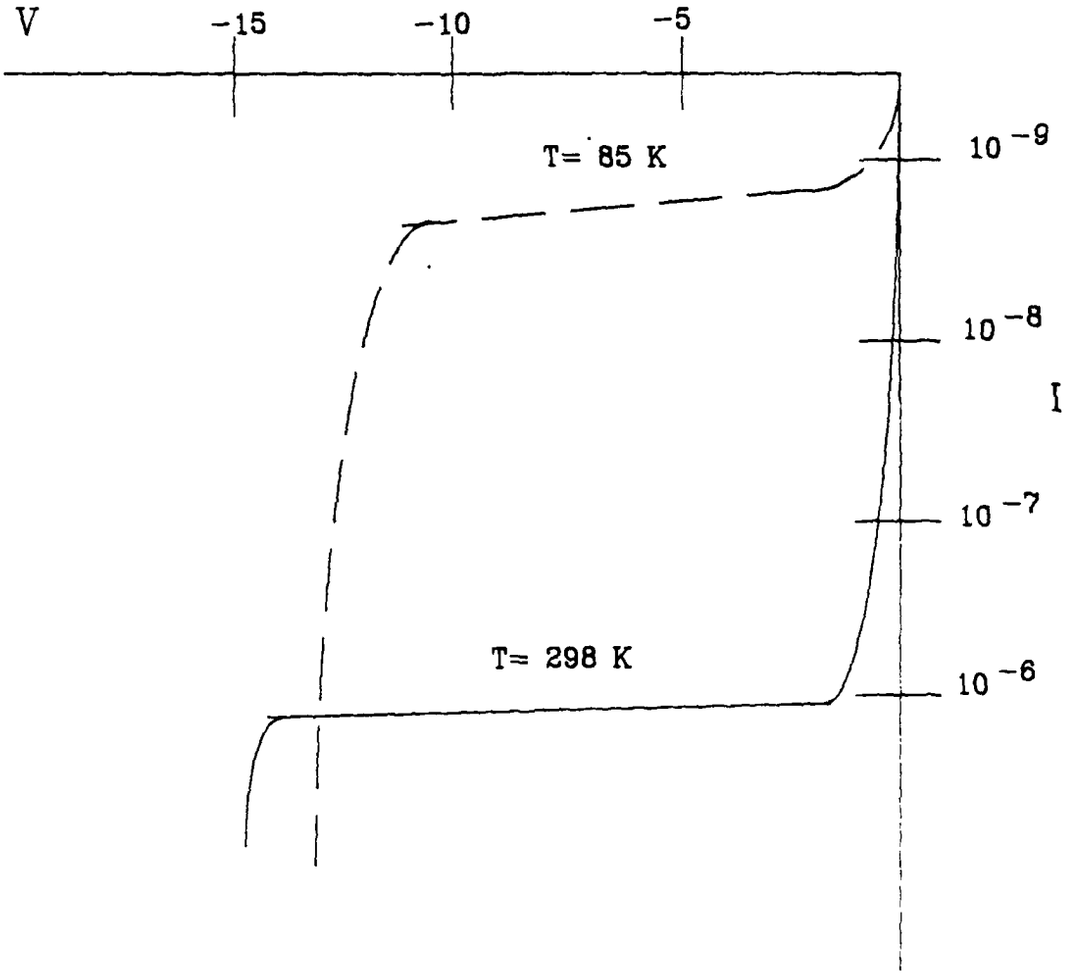

Figure 18. Dark current for diode f at T=85 K and room temperature.

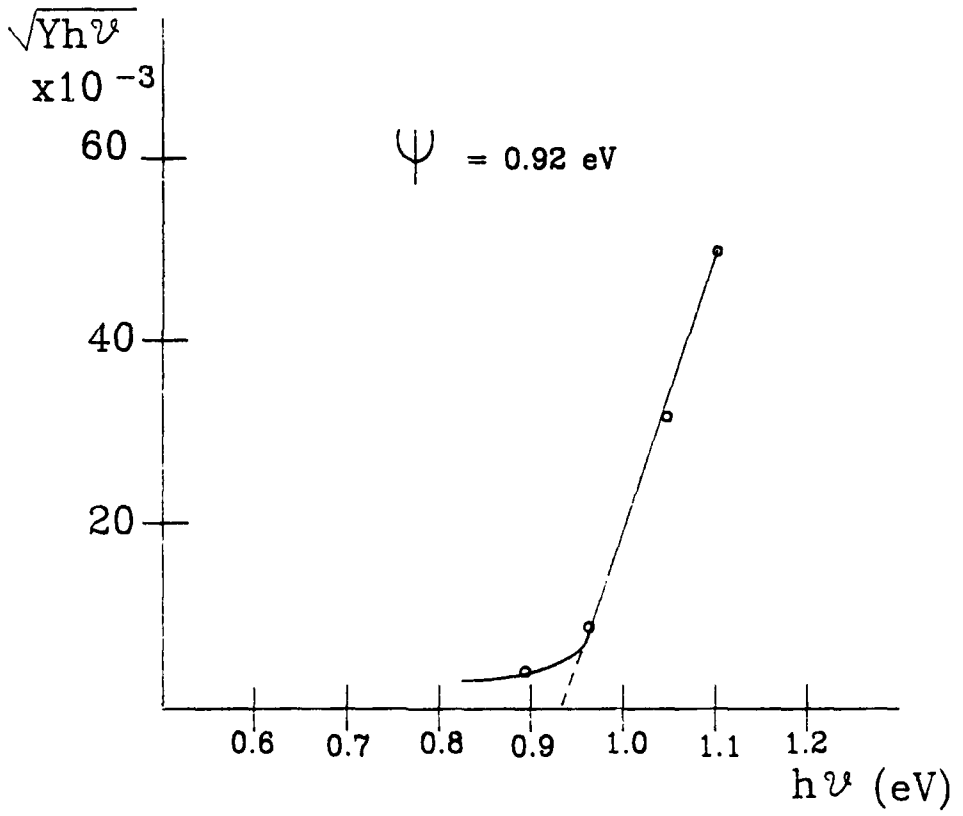

Figure 19. Fowler plot showing barrier height of PtSi diode.

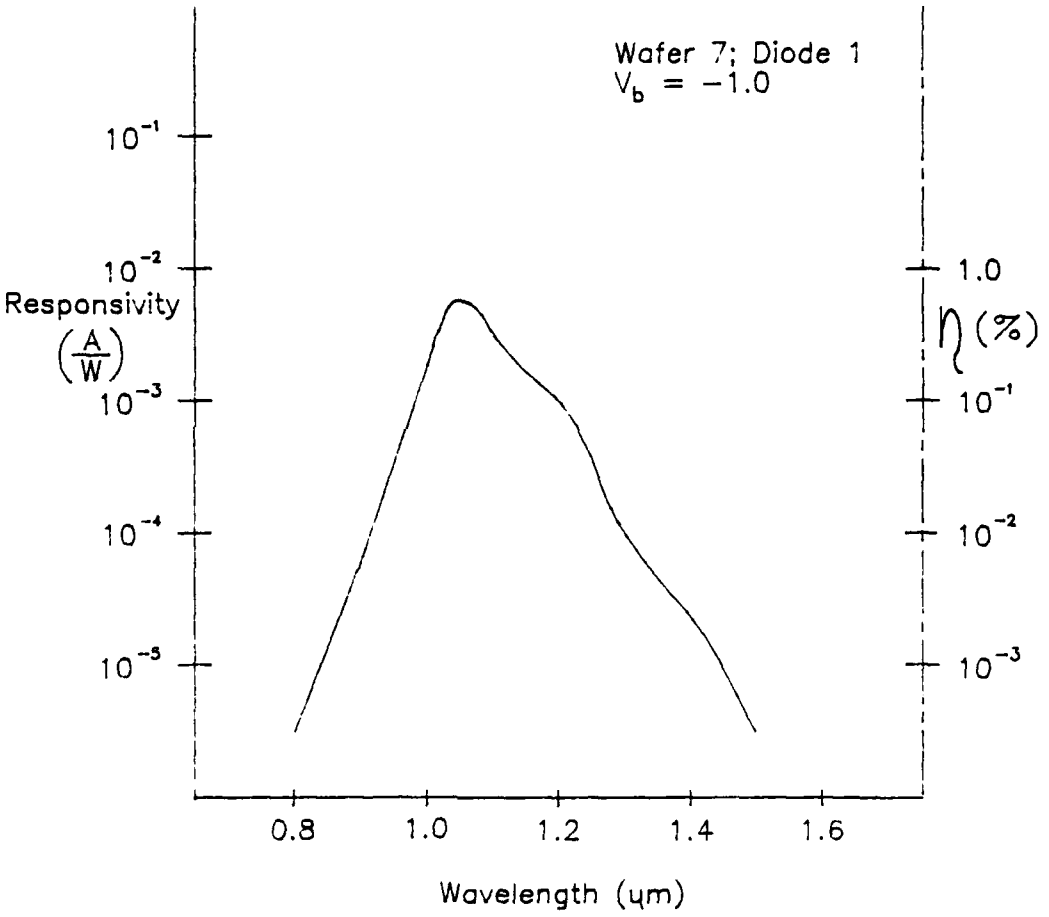

Figure 20. Responsivity and quantum efficiency versus wavelength diode e.

band. However, avalanche multiplication would increase the effectiveness of the quantum efficiency by $M\eta$. In addition, increasing the bias to operate at avalanche will lower the Schottky barrier (see equation 2.4) and allow electrons to pass over the barrier that were unable to do so at the lower reverse bias. The detector would therefore be feasible for operation at the shorter wavelength end of the desired optical band of 1.3 - 1.6 μm.

The reverse breakdown voltage for these diodes is shown in figures 16, 17, and 18. The values range from 6 to 14 volts, which is relatively low. The donor concentration can be varied to adjust the breakdown voltage, whereby a decrease in the donor concentration increases the breakdown voltage.[8] Low breakdown voltages are desirable for low noise, because avalanching would occur at voltage below the breakdown voltage of the guard ring. Unfortunately, the low voltages had an adverse effect on the multiplication process.

Avalanche multiplication is determined by measuring the chopped photocurrent at low bias and then comparing it to the chopped signal as the reverse bias is increased up to breakdown voltage. Figure 21 shows the multiplication as a function of reverse bias. As can be seen, the multiplication effect did not materialize. The slight increase in the photocurrent can be attributed to the lowering of the Schottky barrier, but not from impact ionization. The key to the negative results was hinted in the preceding paragraph. *The low breakdown bias contributes to an electric field strength which is too low for photogenerated impact ionization to occur.* The electric field required to produce ionization in silicon is $\cong 3 \times 10^5 \frac{V}{cm}$.[8] By calculating the depletion width for a Schottky diode,

$$W(cm) = \sqrt{\frac{2\epsilon_S}{qN_D}\left[V_{bi} - V - \frac{kT}{q}\right]} \qquad 5.1$$

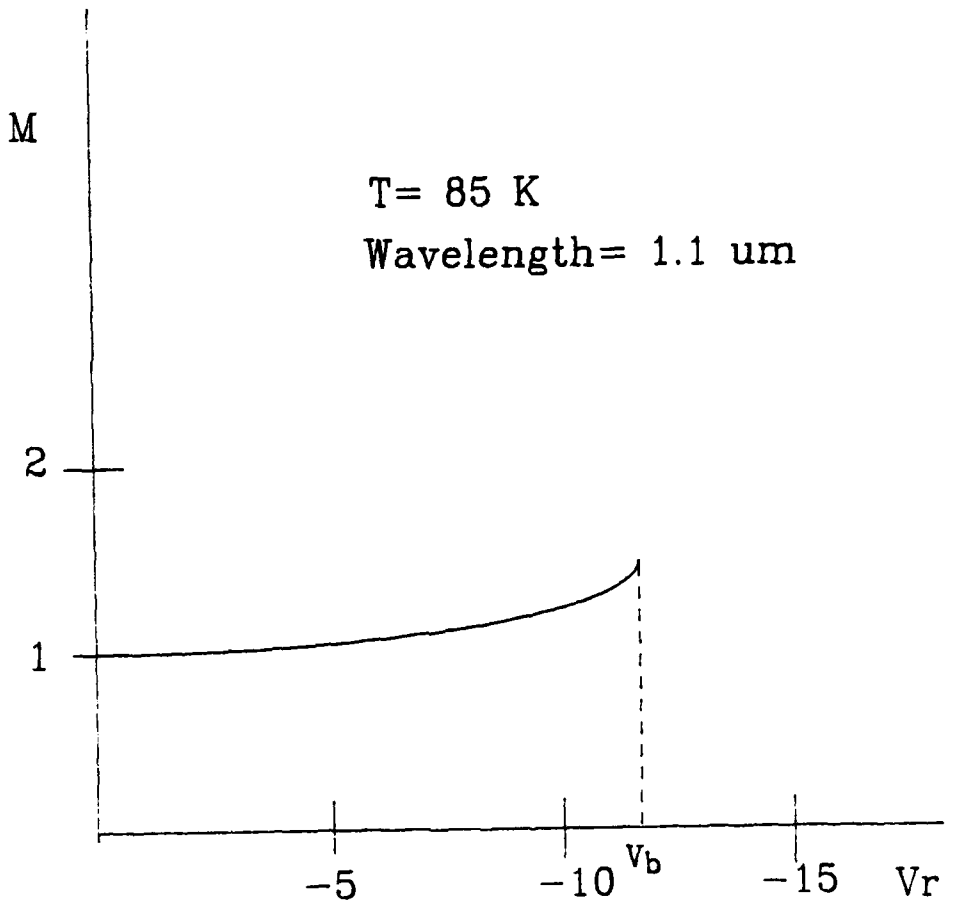

Figure 21. Multiplication versus reverse bias for PtSi diode f.

V_{bi} = built in potential (≅ 0.9 eV)

V = reverse bias

one can estimate the electric field strength by assuming a constant field across the depletion region. At V = -14 volts, V_{bi} = 0.9 volts, N_D =10^{15} cm^{-3}, and T = 85° K, the depletion width is approximately 4.5 μm. Then $\xi = \frac{14}{4.5 \times 10^{-4}} = 3.11 \times 10^4 \frac{V}{cm}$. The electric field is an order of magnitude too low to cause photogenerated impact ionization, and therefore no multiplication effects were observed. Data from Sze shows that for silicon abrupt p-n junctions, with $N_D = 10^{15} cm^{-3}$, the reverse breakdown normally occurs around 300 volts[8] , much larger than the observed 14 volts in the PtSi diodes. Since no multiplication occured, no anlaysis of the excess-noise factor can be made.

Although the low breakdown voltage of the PtSi diodes prevented experimental analysis of the multiplication effects, a prediction of their performance can be made based on the 1967 results of Lepselter and Sze.[27] They analyzed PtSi-Si diodes and found that the reverse breakdown of the diode could approach theoretical predictions for abrupt p-n junctions by implanting a guard ring. With the guard ring and a doping level of 2 x 10^{16} cm^{-3}, they were able to achieve a reverse breakdown of 42 volts with a corresponding 3 μm wide depletion region. This would improve the chances for photogenerated impact ionization. Based on the following parameters, estimations for the multiplication and excess noise for pure electron injection (equations 3.11 and 3.19, respectively) can be calculated:

$\xi = 3 \times 10^5 \frac{V}{cm}$

$\alpha = 7.32 \times 10^3$ cm^{-1} [ref 21, p. 381]

$\beta = 1.01 \times 10^3$ cm^{-1} [ref 21, p. 381]

$k = \frac{\beta}{\alpha} = 0.138$

$W = 3\ \mu m$

Therefore, $M_n \cong 68$ with $F_n \cong 11.1$ for pure electron injection ($\psi < h\nu < E_g$). Figure 22 shows values of F_n versus M_n out to $M_n = 68$ and $k = 0.138$. To get an idea of the performance of the detector, we can use our estimated values of M_n and F_n to determine the Noise Equivalent Power of the detector from equation 3.5 and 3.6 by setting the $\frac{S}{N} = 1$. With negligible background current and $M_n = 68$, equation 3.6 reduces to $I_{eq} \cong I_{Db}F_n$, where I_{Bd} is the bulk dark current. As stated earlier, the bulk dark current can be an order of magnitude lower than the surface dark current. Therefore, if at room temperature the total dark current is 1 μA, then the bulk dark current may be only 0.1 μA. Then the NEP from equation 3.5 would be appoximately 2.5×10^{-8} watts at 1.3 μm, $\eta = 0.01$ percent, B = 10 Hz. This figure could be improved by cryogenic cooling to reduce the dark current.

The gain-bandwidth product can also be estimated using equation 3.13 and the following values: N = 1, W = 3 μm, $v_n = 10^7 \frac{cm}{s}$, $\frac{\beta}{\alpha} = 0.138$. Therefore, $M(\omega)\omega = 2.42 \times 10^{11}$. If $M(\omega) = 68$, then the bandwidth would be 3.55 GHz.

Another alternative to the problem of the low reverse breakdown in the PtSi diode would be to increase the doping concentration to 10^{17} cm^{-3} and cool the detector to T = 10°K, and thus use impurity-band ionization instead of valence-to-conduction band ionization. At the lower required electric field, the 14 volt reverse bias would produce ample electric field strength to cause impurity-band ionization and thus multiplication.

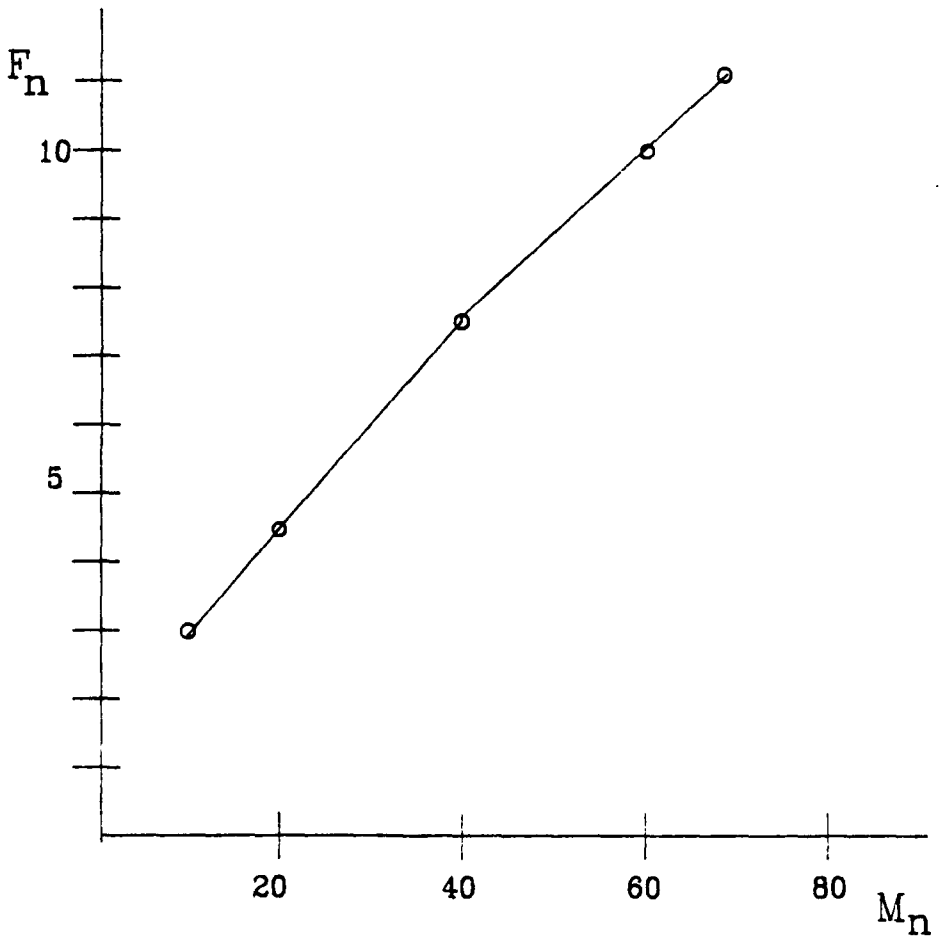

Figure 22. Fn versus Mn for predicted performance of PtSi diodes.

CHAPTER 6

CONCLUSIONS

Fiber optic communication systems have been the driving force for developing detector technology for the 1.3 to 1.6 micron region. The PtSi Schottky Barrier Diode was investigated because of its spectral response and compatibility with monolithic construction. The physics of the barrier formation and current transport properties were discussed in order to understand the operating principles of the diode. The barrier height, and thus the spectral response, is determined primarily by the work functions of the metal and semiconductor used.

Because the operating environment consists of wide bandwidth-high frequency applications, operation in the avalanche mode was considered. An avalanching detector should be used when the system is limited by thermal or amplifier noise. The signal and noise are then multiplied above the thermal or amplifier noise while introducing as little additional noise as possible, thereby maintaining the signal-to-noise ratio. How much multiplication will occur is dependant mainly on the ionization coefficients of the holes and electrons and diode construction. The best situation is when α and β differ greatly and when the multiplication is initiated by the carrier with the higher ionization coefficient. Thus in silicon, where $\alpha > \beta$, the multiplication should be initiated by electrons. By using the PtSi Schottky diode construction and operating in the spectral region of $\psi < h\nu < E_g$, we can theoretically achieve pure electron injection, and thus take advantage of the higher electron ionization coefficient.

Experimental results for the PtSi diodes studied showed high dark currents (1μA) at room temperature, reduced to 1 nA at 85^0 K, and reverse breakdown voltages (6 to 14 volts) that were too low to cause photon generated multiplication. However, predictions can be made on the performance of the PtSi diodes as reported by Lepselter and

Sze. With doping levels of $2x10^{16}$ cm^{-3} and reverse breakdown at 43 volts, multiplication of approximately 68 with an excess-noise factor of 11.1 can be achieved operating at 1.3 microns. An alternative option would be to use impurity-band impact ionization by heavily doping with impurities and operating at low temperatures. Based on these predictions, the PtSi diode should be considered a viable candidate for detectors in fiber optic systems.

REFERENCES

1. J.C. Cambell, "Photodetectors and Compatible Low-Noise Amplifiers for Long-Wavelength Light Wave Systems," *Fiber and Integrated Optics*, 5, 1(1984).

2. T. Mikawa, S. Kagawa, and T. Kaneda, "Germanium Reachthrough Avalanche Photodiodes for Optical Communication Systems at 1.55 μm Wavelength Region," *IEEE Trans. Elect. Dev.*, **ED-31**, 971 (1984).

3. F. Braun, "Uber die Stromleitung durch Schwefelmetable," *Amn. Phy. Chem.*, **153**, 556 (1874).

4. J.C. Bose, U.S. Patent 775,840 (1904).

5. A.H. Wilson, "The Theory of Electronic Semiconductors," *Proc. R. Soc. Lond. Ser. A*, **133**, 458 (1931).

6. W. Schottky, "Halbleitertheorie der Sperrschicht," *Naturwissenschaften*, **26**, 843 (1938).

7. L. Scholnik, et al, "A Schottky Barrier Monolithic IRCCD Focal Plane," *Proceedings of the 27th National IRIS*, U.S. Naval Training Center, San Diego, Ca., May 15-17, 1979.

8. S.M. Sze, *Physics of Semiconductor Devices*, 2nd ed. (John Wiley and Sons, New York, 1981).

9. E.L. Dereniak and D.G. Crowe, *Optical Radiation Detectors*, (John Wiley and Sons, New York, 1984), p. 75.

10. R. Taylor, et al, "Improved Platinum Silicide IRCCD Focal Plane," *SPIE*, **217** (1980).

11. W.F. Kosonocky, et al, "Schottky-Barrier Infrared Image Sensors," *RCA Engineer*, 27-3, 50 (1982).

12. J.M. Mooney and J. Silverman, "The Theory of Hot-Electron Photoemission in Schottky-Barrier IR Detectors," *IEEE Trans. Elect. Dev.*, **ED-32**, 33 (1985).

13. J.M. Mooney, "Internal Photoemission in Platinum Silicide Schottky Barrier Infrared Photodetectors," PhD dissertation, University of Arizona, Optical Sciences Center, 1986.

14. G.E. Stillman and C.M. Wolfe, in *Semiconductors and Semimetals*, edited by R.K. Willardson and A.C. Beer, (Academic Press, New York, 1977), vol 12.

15. P.P. Webb, R.J. McIntrye, and J. Conradi, "Properties of Avalanche Photodiodes," *RCA Review*, **35**, 235 (1974).

16. W. Schockley, *Solid State Electronics*, **2**, 36 (1961).

17. H. Kressel, *RCA Review*, 28, 175 (1967).

18. H. Melchior and W.T. Lynch, "Signal and Noise Response of High Speed Germanium Avalanche Photodiodes," *IEEE Trans. Elect. Dev.*, ED-13, 832 (1966).

19. R.J. McIntyre, "Multiplication Noise in Uniform Avalanche Diodes," *IEEE Trans. Elect. Dev.*, ED-13, 166 (1966).

20. R. Chin, "GaAlAsSb APD Optimization," RADC-TR-84-191 Final Technical Report, Rome Air Development Center, Air Force Systems Command, Oct. 1984.

21. M.H. Woods, W.C. Johnson, and M.A. Lampert, "Use of a Schottky Barrier to Measure Impact Ionization Coefficients in Semiconductors," *Solid State Electronics*, 16, 383 (1973).

22. N.F. Mott and W.D. Twose, *Adv. Phys.*, 10, 107 (1961).

23. M.D. Petroff, et al, "Detection of Individual 0.4-28 μm Photons Via Impurity-band Ionization in a Solid-State Photomultiplier," *Appl. Phys. Lett.*, 51, 406 (1987).

24. D.E. Gray, ed., *American Institute of Physics Handbook*, (McGraw-Hill Book Co., New York, 1972), p. 7-10.

25. F. Capasso, et al, "New Avalanche Multiplication Phenomenon in Quantum Well Superlattices: Evidence of Impact Ionization Across the Band-Edge Discontinuity," *Appl. Phys. Lett.*, 48, 1294 (1986).

26. E.L. Dereniak and C.T. Willoughby, "Investigation of Silicide Schottky Barrier Diodes," Optical Sciences Center, University of Arizona, prepared for Solid State Sciences Division, Rome Air Development Center, Sep. 30, 1986.

27. M.P. Lepselter and S.M. Sze, "Silicon Schottky Barrier Diode with Near-Ideal I-V Characteristics," *The Bell Systems Technical Jounal*, Feb. 1968.

28. L.K. Anderson and B.J. McNartry, *Proc. IEEE*, 54, 1335 (1966); L.K. Anderson, M DiDomenico Jr., and M.B. Fisher, *Advan. Microwaves*, 5 (1970).